Satellite Data for U.S. Air Quality Applications: *Examples of Applications, Summary of Data End-User Resources, Answers to FAQs, and Common Mistakes to Avoid*

Bryan N. Duncan[1], Ana I. Prados[1,2], Lok Lamsal[1,3], Yang Liu[4], David Streets[5], Pawan Gupta[1,3], Ernest Hilsenrath[2,6], Ralph Kahn[1], J. Eric Nielsen[7], Andreas Beyersdorf[8], Sharon Burton[8], Arlene M. Fiore[9], Jack Fishman[10], Daven Henze[11], Chris Hostetler[8], Nickolay A. Krotkov[1], Pius Lee[12], Meiyun Lin[13], Steven Pawson[1], Gabriele Pfister[14], Kenneth E. Pickering[1], Brad Pierce[15], Yasuko Yoshida[1,7], Luke Ziemba[8]

[1]NASA Goddard Space Flight Center, Greenbelt, MD, USA
[2]Joint Center for Earth System Technology, University of Maryland, Baltimore County, Baltimore, MD, USA
[3]Goddard Earth Sciences Technology and Research, Universities Space Research Association, Columbia, MD, USA
[4]Emory University, Rollins School of Public Health, Atlanta, GA, USA
[5]Argonne National Laboratory, Argonne, IL, USA
[6]Sigma Space Corporation, Lanham, MD, USA
[7]Science Systems and Applications, Inc., Lanham, MD, USA
[8]NASA Langley Research Center, Hampton, VA, USA
[9]Lamont-Doherty Earth Observatory of Columbia University, Palisades, NY, USA
[10]St. Louis University, St. Louis, MO, USA
[11]University of Colorado, Boulder, CO, USA
[12]National Oceanic and Atmospheric Administration, Silver Spring, MD, USA
[13]Princeton University, Princeton, NJ, USA
[14]National Center for Atmospheric Research, Boulder, CO, USA
[15]National Oceanic and Atmospheric Administration, Madison, WI, USA

*Corresponding author: Bryan N. Duncan, Code 614 NASA Goddard Space Flight Center, Greenbelt, MD 20771, USA. Email: Bryan.N.Duncan@nasa.gov. Phone: 1-301-614-5994; Fax: 1-301-614-5903.

Abstract.

Satellite data of atmospheric pollutants are becoming more widely used in the decision-making and environmental management activities of public, private sector and non-profit organizations. They are employed for estimating emissions, tracking pollutant plumes, supporting air quality forecasting activities, providing evidence for "exceptional event" declarations, monitoring regional long-term trends, and evaluating air quality model output. However, many air quality

managers are not taking full advantage of the data for these applications nor has the full potential of satellite data for air quality applications been realized. A key barrier is the inherent difficulties associated with accessing, processing, and properly interpreting observational data. A degree of technical skill is required on the part of the data end-user, which is often problematic for air quality agencies with limited resources. Therefore, we 1) review the primary uses of satellite data for air quality applications, 2) provide some background information on satellite capabilities for measuring pollutants, 3) discuss the many resources available to the end-user for accessing, processing, and visualizing the data, and 4) provide answers to common questions in plain language.

Keywords: satellite data; air quality; end-user resources; remote sensing

Table of Contents

1. Introduction 5
2. Current satellite data applications in the U.S. 6
2.1 Tracking pollutant plumes 6
Case Example #1: Pollution transport during the NASA DISCOVER-AQ field campaign . 7
2.2 Support for AQ forecasting 8
2.3 Evidence for exceptional event demonstrations 9
Case Example #2: Wildfires enhance aerosols in Virginia, North Carolina and California 10
Case Example #3: Periodic surface ozone enhancement from stratospheric intrusions 11
2.4 Evaluating output of models and providing input to models 13
3. Potential satellite data applications in the U.S. 13
3.1 Estimating anthropogenic pollutant emissions 13
3.2 Monitoring long-term trends of ambient pollutant concentrations 15
4. Data basics, including processing and visualization resources 16
4.1 Levels of data and spatial resolution 17
4.2 Temporal resolution and latency 17
4.3 Access to data files 18
4.4 Visualization and analysis tools 18
4.4.1 Gas and aerosol products 19
4.4.2 Near-real-time true color imagery and fire products 20
4.4.3 Exceptional Event Decision Support System (EE DSS) 20
5. Straight answers to frequently-asked questions (FAQs) 21
5.1 Can satellites measure “nose-level” concentrations? 21
5.1.1 Are there satellite data for surface ozone? 21
5.1.2 Are there satellite data for surface NO_2? 22
5.1.3 Are there satellite data for surface VOCs? 23
5.1.4 Are there data for surface CO? 24
5.1.5 Are there data for surface SO_2? 24
5.1.6 Are there data for surface $PM_{2.5}$? 24
5.2 Why are there multiple products for the same species? 25
5.2.1 Why are there multiple products for some species from the same instrument and which should I use for my application? 25
5.2.2 Why are there multiple instruments that measure the same quantity? 26
5.3 Are there data with finer spatial resolution? 26
5.4 Are there data that span the entire day? 27
5.5 How does a satellite instrument measure gases and aerosols? 28
5.6 How does one quantify the amount of a pollutant in the atmosphere from satellite data? . 28
5.7 Why do some products have higher uncertainties than others? 29
5.8 How do I know if my data are statistically significant and accurate? 30

5.9 What is the best way to evaluate model output with satellite data? 32
5.10 Is it true that satellite data will replace the need for surface observational networks?..... 33
5.11 What new and improved satellite missions are being built?..... 33
5.11.1 What new and improved satellite missions are being built for gases? 33
5.11.2 What new and improved satellite missions are being built for aerosols?..... 34
6. Summary and charge to the applied AQ community..... 35
Acknowledgments..... 36
References..... 37
Appendices..... 45
Appendix A. Satellite prediction of surface $PM_{2.5}$ levels 45
Appendix B. An “apples-to-apples” comparison of model output to satellite VCD data 46
Tables..... 48
Table 1. Frequently used acronyms and terms. 48
Table 2. Data discovery, visualization, and analysis resources for the end-user..... 49
Figures..... 51

1. Introduction

There is now a wealth of atmospheric composition satellite data for air quality (AQ) applications that has proven valuable to environmental professionals: nitrogen dioxide (NO_2), sulfur dioxide (SO_2), ammonia, carbon monoxide (CO), some volatile organic compounds (VOCs), and aerosol optical depth (AOD), from which surface particulate matter ($PM_{2.5}$) may be inferred. The National Aeronautics and Space Administration (NASA) Applied Sciences Program, within NASA's Earth Science Division, initiated two programs to promote and facilitate the use of these satellite data in the decision-making and environmental management activities of public, private sector and non-profit organizations, such as the Environmental Protection Agency (EPA), state AQ agencies, the American Heart Association, public utilities and other for profit entities, and Non-Governmental Organizations (NGOs). In 2008, the Applied Remote SEnsing Training (ARSET) program (http://airquality.gsfc.nasa.gov/) began providing in-person and on-line AQ courses, workshops and other capacity building activities for end-users. Since then, the program has expanded to include water resources and disaster management. In 2010, the Air Quality Applied Sciences Team (AQAST; http://acmg.seas.harvard.edu/aqast/) began to directly engage the management of end-user organizations, serving their applied research needs with a combination of satellite data, suborbital measurements, and computer models.

A barrier to using satellite data for AQ applications is the inherent difficulties associated with accessing, processing, and properly interpreting NASA's observational data. The complementary ARSET and AQAST programs recognize that a degree of technical skill is required on the part of the data end-user, which is often problematic for organizations with limited resources. Therefore, the purpose of this review article, a joint AQAST and ARSET effort, is to inform current and potential end-users of 1) how data are being used by the environmental community for AQ applications (Sections 2 and 3), 2) what resources are available for accessing and processing the data (Section 4), and 3) straight answers in plain language to frequently asked questions, including common mistakes to avoid when working with data (Section 5). Refer to **Table 1** for a list of acronyms that are frequently used in this article and **Table 2** for web-based data access and visualization tools available to the end-user. We refer the reader to Table 1 of Streets et al. (2013) and Table 1 of Kahn (2012) for a list of the main satellite gas and aerosol products relevant for AQ applications.

The intended audience of this review article is AQ managers and other environmental professionals, particularly those who do not currently use satellite data for their AQ applications, but wish to, or do so sparingly. There are other informative review articles on various aspects of the use of satellite data for AQ applications that will provide additional information to the uninitiated end-user. Examples are Fishman et al. (2008) on the current capabilities of satellite instruments to measure pollutants and Streets et al. (2013) on the use of satellite data for estimating surface emissions of pollutants. The National Science and Technology Council (NSTC) also provides an overview of satellite observations relevant to AQ applications (NSTC, 2013). The instructive review articles of Martin (2008) and Hoff and Christopher (2009) are more technical in their discussions and, therefore, more appropriate for the intermediate and advanced satellite data end-user. Ichoku et al. (2012) provide a comprehensive, but technical, overview of using satellite data to characterize various properties of wildfires, such as emission strength and plume rise.

2. Current satellite data applications in the U.S.

The successful uses of satellite data for AQ applications all take advantage of the primary strength these products have over the conventional ground-based monitoring networks - spatial coverage (e.g., **Figure 1**). EPA and many state AQ agencies recognize the utility of satellite data for AQ applications and some of them are actively considering how they can be further used for monitoring and regulatory purposes. We identified six main categories of current and potential applications: tracking pollutant plumes, support for AQ forecasting, evidence in exceptional event demonstration packages submitted to EPA, input to AQ models and data for model evaluation, estimating ozone precursor and aerosols emissions, and monitoring regional long-term trends in ozone precursors and aerosols. In this review, we do not discuss the many ways that meteorological satellite data are used in AQ applications. Instead, we focus on variables from satellite data that provide information on the distributions of pollutants and pollutant emissions.

2.1 Tracking pollutant plumes

Over the last decade, satellite data have been used widely to track pollution from agricultural and wild fires. As illustrated in *Case Example #1*, satellite data provide important information

on pollution characteristics, including its composition, accumulation over regions, and long-range transport.

Case Example #1: **Pollution transport during the NASA DISCOVER-AQ field campaign**

Agricultural fires occur annually in late summer and early fall in the Mississippi River Valley (e.g., Korontzi et al., 2008). In mid-September 2013, pollution from these fires reached Houston, Texas, during the NASA DISCOVER-AQ (Deriving Information on Surface conditions from Column and Vertically Resolved Observations Relevant to Air Quality) field campaign. The goal of the campaign was to collect targeted airborne and ground-based observations of pollutants to enable more effective use of satellites to diagnose "nose-level" AQ. Participants in the campaign coordinated the mission with personnel of the Texas Commission on Environmental Quality (TCEQ).

Data from the Visible Infrared Imaging Radiometer Suite (VIIRS), which measures AOD on the Suomi National Polar-orbiting Partnership (NPP) satellite, indicate that aerosol levels were regionally high over the southern U.S. (**Figure 2a**). AOD is the degree to which aerosols prevent the transmission of light by absorption or scattering of light through the entire vertical column of the atmosphere from the ground to the satellite's sensor. The terms "aerosol" and "particulate matter" are often used interchangeably and refer to suspensions of solid or liquid particles in air, though particulate matter is usually associated with a specific particle size range, such as < 2.5 μm for $PM_{2.5}$ and < 10 μm for PM_{10}.

For several days, aerosol levels increased over the southern U.S. as a result of smoke from the agricultural fires that mixed with other anthropogenic aerosols. A "backdoor" cold front transported the aerosols to the west and southwest as indicated by the VIIRS AOD product and reached the Houston metropolitan area on September 14th (**Figure 2a**). Enhanced AOD levels were generally between 0.4 and 0.6 throughout the day and twice as high as previous days. They were confirmed by data from NASA's ground-based DRAGON (Distributed Regional Aerosol Gridded Observational Network; Holben et al., 1998, 2001) network of sun photometers which measure the same quantity as the satellite-derived AOD.

However, surface data from the TCEQ observational sites show that $PM_{2.5}$ levels remained relatively low (< 25 μg/m^3) in the metropolitan area on September 14th, indicating that much of the imported pollution was located above the area. Data collected by the NASA High Spectral

Resolution Lidar-2 (HSRL-2) instrument (Hair et al., 2008; Hostetler et al., 2012), which was on board an aircraft as part of the DISCOVER-AQ mission, confirm that a layer of aerosols was located >1 km above the surface (**Figure 2b**).

Interestingly, the ambient extinction coefficients (i.e., a measure of how strongly air and aerosols absorb and scatter light at a particular wavelength) in this layer were nearly two times higher than the dry extinction coefficients as measured by a particle soot absorption photometer (PSAP) and two parallel nephelometers on the DISCOVER-AQ aircraft. This indicates that high relative humidity enhanced the scattering of light by the aerosols and, thus, increased AOD (**Figure 2c**; Ziemba et al., 2013). For further information on the complex relationship between satellite-derived AOD, relative humidity, and surface $PM_{2.5}$, see Hoff and Christopher (2009) and Ziemba et al. (2013). As discussed by Hoff and Christopher (2009), unless the aerosol loading is concentrated at the surface, deriving surface $PM_{2.5}$ from satellite AOD requires additional information on the vertical aerosol distribution from a chemical transport model or a lidar instrument (see Section 5.1.6).

While the agricultural fire pollution did not elevate $PM_{2.5}$ levels at the surface in Houston, it did several kilometers above the city and at the surface in the Mississippi Valley. This case example illustrates 1) the complementary nature of the satellite observations to data collected by surface AQ monitors, 2) the power of satellite data to provide an overview of the regional buildup and the long-range transport of pollution, which can degrade AQ far downwind, 3) the limitations of the satellite data (e.g., the lack of information on the vertical distribution and chemical composition of the aerosols, and gaps in spatial coverage due to clouds), and 4) the complicated relationship between AOD, relative humidity, and $PM_{2.5}$, showing that high AOD values do not necessarily translate to high surface $PM_{2.5}$ levels (e.g., Ziemba et al., 2013) – a common mistake to avoid.

2.2 Support for AQ forecasting

One of the most frequent applications of satellite data in the U.S is for AQ forecasting support. NASA imagery is often accessed on a daily basis by state AQ agencies across the U.S., such as the Virginia Department of Environmental Quality (DEQ), the Idaho DEQ, and the California Air Resources Board (CARB). For instance, the Idaho DEQ recently attended an ARSET training course in Madison, Wisconsin (NASA Applied Sciences Annual Report, 2012). As a

result, they used NASA imagery to support their AQ forecasts during the summer wildfire season of 2012. Each day, staff at the DEQ combined NASA satellite data with surface monitor information to produce a daily report that was forwarded to the forecasters. The information in the report included MODIS smoke imagery, AIRS CO layers, and fire detection maps downloaded from NASA web tools and then imported into geographic information systems (GIS).

The use of satellite data for AQ forecast support is generally qualitative, such as imagery which has a natural color rendition similar to a photograph (i.e., true color imagery), daily AOD from satellites, or daily CO and smoke extent maps during the fire season in states where fires often enhance surface $PM_{2.5}$ levels. Two of the most popular web tools among AQ forecasters are the National Oceanic and Atmospheric Administration (NOAA) Infusing Satellite Data into Environmental Applications (IDEA) web tool and the NOAA Hazard Mapping System Fire and Smoke Product (HMS). See Section 4 for more details on these two web tools.

2.3 Evidence for exceptional event demonstrations

Section 319 of the Clean Air Act defines an event as exceptional "if the event affects air quality; is an event that is not reasonably controllable or preventable; is an event caused by human activity that is unlikely to recur at a particular location or a natural event; and is determined by EPA to be an exceptional event". It also "requires a State air quality agency to demonstrate through reliable, accurate data that is promptly produced that an exceptional event occurred" and that "a clear relationship be established between a measured exceedance of a NAAQS and the exceptional event…" (Federal Register, 2007). These "exceptional events" may be exempted by EPA from counting towards regulatory decisions, such as non-attainment determinations. The "weight of evidence" presented in the exceptional event demonstration submission to EPA may include data from surface monitors and satellites alongside model simulations that clearly demonstrate that the exceedances of the NAAQS threshold would not have occurred "but for" the exceptional event. Exceptional events include, for example, dust storms, wild fires and fireworks.

State AQ agencies commonly use satellite imagery to illustrate fire locations, pollutant transport due to wildfires and associated meteorological phenomena, such as frontal boundaries or storm systems. The ARSET program receives frequent requests from state and local

regulatory agencies seeking to acquire the skills to use satellite data for exceptional event demonstrations, and, in particular, long-range transport of aerosols from wildfires and dust, and ozone exceedances at the surface due to stratospheric intrusions of ozone-rich air in the western U.S. Until recently, NASA Terra and Aqua Moderate Resolution Imaging Spectroradiometer (MODIS) true color imagery and AOD data from NOAA's Geostationary Operational Environmental Satellite (GOES) Aerosol/Smoke Product (GASP; Knapp et al., 2005; Prados et al., 2007) have been the main image types used in exceptional event demonstrations. In addition to aerosols, satellite instruments are able to detect the number of molecules of some gases between the instrument and the Earth's surface; this quantity is typically referred to as a "vertical column density" (VCD) in units of molecules per unit area of the Earth's surface. The two principal VCD products provided by NASA for AQ applications are CO and NO_2. Ozone VCD data have also been included in exceptional event submissions to EPA as discussed below; however, they were not used to demonstrate high surface ozone levels since surface ozone cannot be discriminated from these data (see Section 5.1.1). Here we provide a few examples of NASA data used in exceptional event demonstrations. The reader is referred to the AQAST website for more information on how current AQAST members are helping AQ agencies to prepare their exceptional event demonstrations (e.g., Fiore et al., 2014).

Case Example #2: **Wildfires enhance aerosols in Virginia, North Carolina and California**

Wildfires can have a significant impact on AQ by enhancing the surface concentrations of aerosol and precursors to ozone formation. The key challenge for regulators is demonstrating that the exceptional event caused a specific air pollution concentration at a particular location. A number of AQ agencies regularly use MODIS true color imagery in their exceptional event demonstration packages to help illustrate aerosol transport patterns. However, true color images alone do not provide quantitative information such as aerosol concentrations nor do they provide plume height information. In general, it is more difficult to quantify the impact of wildfires on ozone as ozone formation can occur far downwind of the fires (e.g., Fiore et al., 2014) where AQ may already be poor in the absence of the fires, particularly in hot weather. An additional challenge for exceptional event demonstrations is that wildfire pollutant emissions can vary dramatically in time and space and depend on the type and condition of the fuel burned.

While wildfires are more prevalent in the western U.S. and agricultural fires (e.g., **Figure 2**) are prevalent in the central and southern U.S., wildfires do periodically impact AQ in the eastern U.S. For example, **Figure 3** shows a Terra MODIS true color image of smoke from the Great Dismal Swamp wildfire in Virginia and the Evans Road wildfire in North Carolina in June 2008. Similar images were submitted in exceptional event demonstration packages to EPA for this event by the Virginia Department of Environmental Quality (VA DEQ), the Maryland Department of the Environment (MDE), and the North Carolina Department of Environment and Natural Resources (NC DENR). The exceptional event demonstration package from MDE also included satellite data of the vertical distribution of aerosols from the NASA Cloud-Aerosol Lidar and Infrared Pathfinder Satellite Observation (CALIPSO) instrument as well as AOD data from the Aqua MODIS instrument. **Figure 3** also shows a MODIS Aqua true color image of wildfire smoke that affected much of northern California during the summer of 2008. The season started with the Northern California Lightning Siege (or the Lightning Complex Fires) on June 20-22, when lightning strikes led to one of the most intense and lengthy fire seasons in California history. In their exceptional event demonstration package, the California Air Resources Board (CARB) submitted numerous MODIS true color images for June 20th – August 16th, 2008.

Case Example #3: **Periodic surface ozone enhancement from stratospheric intrusions**

Recent observational and modeling studies show that stratospheric air can "fold" into the troposphere and descend to the surface, episodically pushing ground-level ozone over the National Ambient Air Quality Standard (NAAQS) threshold at elevated western U.S. sites (Langford et al., 2009, 2012; Lefohn et al., 2011; Lin et al., 2012; Yates et al., 2013). These "stratospheric intrusions" will more frequently lead to ozone NAAQS exceedances as the ozone standard is lowered. Consequently, the EPA recently formed a working group of scientists and AQ managers from local, state, and federal agencies with the purpose of providing support for the identification of an intrusion, using a combination of models, surface observations, and satellite data.

Relative to surface air, stratospheric air has lower moisture and CO concentrations, but higher ozone concentrations. These characteristics can be used to identify intrusions, which typically occur in spring and are associated with storm systems. However, the identification of intrusions

is challenging given their episodic, transient and localized nature and the limited spatial and temporal extent of surface measurements available to diagnose their presence. Therefore, data from surface monitors, ozonesondes, and satellites together with model simulations can help demonstrate whether an intrusion is the primary cause of an exceedance of the NAAQS for ozone (e.g., Lin et al., 2012).

Figure 4 illustrates the power of a model to demonstrate when an intrusion enhances surface ozone levels. An intrusion that impacted several states from February 27-28th, 2009 is clearly shown in output from the NASA Goddard Earth Observing System version 5 (GEOS-5) chemistry and climate model (Pawson et al., 2008; Rienecker et al., 2008; Ott et al., 2010; Molod et al., 2012). The model was used with a horizontal spatial resolution of 25 km x 25 km, which is fine enough for simulating the complex dynamics of a stratospheric intrusion. The figure shows that the 70 ppbv iso-surface of ozone, shown in gray, was in the boundary layer over Oregon and at the surface in Wyoming on February 27th. The model output indicates that stratospheric air impacted surface ozone levels from February 27-28th over a large region, including Oregon, Idaho, Wyoming, Colorado, Arizona, New Mexico, and west Texas.

AQ agencies from two states, Wyoming and Colorado, submitted exceptional event declaration packages to EPA for stratospheric intrusions, including the one illustrated in **Figure 4**. The Wyoming Department of Environmental Quality (DEQ) submitted two exceptional event packages for four intrusion events, using the NASA Aqua Atmospheric Infrared Sounder (AIRS) CO product to demonstrate that the elevated surface ozone was associated with CO-poor air as opposed to CO-rich air influenced by local pollution sources. It also used atmospheric water vapor data in the upper troposphere (i.e., the GOES Band-12 product) to show that the air above the monitoring station was dry, which is characteristic of an intrusion, and AIRS and GOES ozone VCD products to illustrate the sharp horizontal gradient in ozone, which is associated with the synoptic pattern where intrusions typically occur. Similarly, the Colorado Department of Public Health and Environment (CDPHE) used the ozone products from the European Organisation for the Exploitation of Meteorological Satellites (EUMETSAT) Metop-A Global Ozone Monitoring Experiment-2 (GOME-2) and NASA Aura Ozone Monitoring Instrument (OMI) instruments in its exceptional event package.

2.4 Evaluating output of models and providing input to models

Satellite data can be applied in a variety of ways to improve AQ models used to develop State Implementation Plans (SIP). Specifically, they can be used to evaluate the quality of the model-predicted pollutant concentrations and to constrain model input, such as pollutant emissions (e.g., wildfires with fire-counts and fire radiative power data), biogenic emissions of VOCs (e.g., with photosynthetically active radiation and leaf area index data), and photolysis rates (e.g., ozone VCD data). As a specific example, the OMI NO_2 VCD product could be used to evaluate the simulation of NO_x (= NO + NO_2), an important ozone precursor, in the EPA Community Air Quality Model (CMAQ). Such an evaluation may reveal inaccuracies of emissions as well as deficiencies in the chemical mechanism. For instance, a long-standing problem for simulating NO_x is the uncertainties associated with the lifetime and chemical fate of alkyl nitrates (e.g., Kasibhatla et al., 1997).

3. Potential satellite data applications in the U.S.

The next two applications, estimating pollutant emissions (Section 3.1) and monitoring long-term trends (Section 3.2), are actively used by the research community, but are under-used by the applied community. In addition, a third potential application of satellite-derived concentrations is to help guide surface monitor siting by regulatory agencies around new or existing point sources, particularly large NO_x sources.

3.1 Estimating anthropogenic pollutant emissions

As discussed in Section 2.3, satellite instruments are able to detect the number of molecules of a particular gas between the instrument and the Earth's surface - a "vertical column density" (VCD) in units of molecules per unit area of the Earth's surface. If pollution transport, deposition, and chemical conversion are minimal or can be appropriately taken into account, then the observation can reflect the emission rate of the chemical species. The main areas of application and opportunity are NO_x and SO_2 emissions from point sources and NO_x, CO, methane, ammonia, and VOC emissions from area sources. Derivation of surface $PM_{2.5}$ from satellite AOD has been the subject of extensive research (Hoff and Christopher, 2009; Section 5.1.6), but AOD data alone do not provide information on chemical composition or source

emission strength. In the next few paragraphs we highlight a number of recent studies from the scientific literature that have focused specifically on the application of satellite techniques to gas emissions estimation; Streets et al. (2013) provide an in-depth discussion on this topic.

Point sources are natural targets for application of satellite data as entities who own facilities that emit criteria pollutants are subject to emissions verification and compliance. When it comes to SO_2 emissions from coal-fired power plants (e.g., **Figure 5**), considerable ingenuity and statistical data enhancement techniques are needed to draw out the weak signals (see Section 5.7). Fioletov et al. (2011) reported that the detection limit for SO_2 emissions is ~70 gigagrams per year for North American power plants. The instrumental NO_2 sensitivity is much stronger than for SO_2 (Section 5.8), and therefore it is possible to detect emissions from a much wider range of source types. Kim et al. (2006, 2009) and Russell et al. (2012) examine NO_x emissions from U.S. power plants. Duncan et al. (2013) showed that known changes of emissions reported by the Continuous Emissions Monitoring Systems (CEMS) from large power plants are generally consistent with observed changes in the OMI NO_2 product over individual facilities. While time trends are believed to be credible, further research is still needed to develop reliable emission estimates for individual plants.

When sources are many, small, and widespread (i.e. “area sources”), it presents a challenge for traditional emission inventory approaches and an opportunity for the use of satellite data for estimating emissions. With the ability to estimate emissions over a wide area, satellite observations can be used to validate or improve existing inventory approaches. NO_x emissions have received the most attention, with a wide variety of studies using satellite-derived NO_2 VCD data to derive emissions from vehicles (Russell et al., 2012), tar sands operations (McLinden et al., 2012), shipping (de Ruyter de Wildt et al., 2012), and cities as a whole (Beirle et al., 2011), as well as natural sources like lightning (Martin et al., 2007; Bucsela et al., 2010) and soils (Hudman et al., 2012). However, to our knowledge, the studies have not been extended to AQ applications for monitoring or regulation of point source emission trends.

At even larger scales, regional, national, and continental CO emissions from small-scale combustion operations, agricultural burning, forest fires, etc., have been estimated in many studies since the launch of the NASA Terra Measurements of Pollution in the Troposphere (MOPITT) instrument in 1999 (e.g., Hooghiemstra et al., 2012). Two pollutants that are emitted from dispersed sources over wide areas, methane (Bloom et al., 2010) and ammonia (Clarisse et

al., 2009), are being studied because emission inventories are unreliable in their characterization of emissions from rice cultivation, fertilizer application, small-scale oil and gas operations, coal production, etc. The most useful of the VOC species that can be observed from space are formaldehyde and glyoxal, both measured by OMI, because they are chemical products of the oxidation of isoprene, a VOC emitted by vegetation, and therefore indicators of the amount of secondary organic aerosol production (e.g., Palmer et al., 2006).

The ability to construct time trends of inferred emissions at scales from days to years has enabled a number of key indicators of human activity to be observed from space, particularly in relation to area-wide NO_x emissions. Weekly cycles of emissions (Kaynak et al., 2009), the effectiveness of temporary emission controls of about monthly duration (Witte et al., 2009), and the impact of economic recessions on emissions of about yearly duration (Castellanos and Boersma, 2012; Russell et al., 2012) have all been reported in the scientific literature. But these applications are underutilized by environmental professionals. Lamsal et al. (2011) showed that emissions estimates can be rapidly updated, while the laborious process of gathering new source data to update emission inventories can take years.

3.2 Monitoring long-term trends of ambient pollutant concentrations

As a result of environmental regulations (e.g., the 1998 NO_x State Implementation Plan (SIP) Call, the Clean Air Interstate Rule (CAIR), and the Tier 1 and 2 standards of the Clean Air Act Amendments) on point and mobile source emissions, most pollutants that can be measured from space show a significant decrease over the U.S. during the satellite data record (1996-present). These changes are generally consistent with the decreases in surface observations reported by EPA (EPA, 2012). For instance, **Figure 6** illustrates the OMI NO_2 product which shows that NO_2 over the U.S. declined significantly (~30-40%) during both the ozone season (i.e., May-September; **Figure 6a**) and annually (**Figure 6b**) from 2005 to 2012. Russell et al. (2012) used their version of the OMI NO_2 product to infer that NO_x emissions changes from large power plants were variable because of regionally-specific regulations, decreasing by 26±12% from 2005 to 2011. They also estimated an average total reduction of 32±7% in NO_2 for U.S. cities from 2005 to 2011 with a 34% decrease in NO_2 from mobile sources. They attributed part of the observed decline in the data to the turnover in the mobile source fleet and part to the global economic recession that began in 2008. The OMI data also show that emissions of SO_2 and NO_x

have decreased dramatically from coal power plants in the U.S. with the implementation of scrubber technology and emission control devices. Fioletov et al. (2011) found a 40% decline in SO_2 over the largest power plants between 2005 and 2010, which is consistent with the 46% decrease in emissions as reported by CEMS. Duncan et al. (2013) concluded that it is practical to use the OMI NO_2 product to assess changes of emissions from power plants that are associated with the implementation of emission control devices and to demonstrate compliance with environmental regulations. The cumulative data records from four similar sensors (i.e., European Remote Sensing (ERS-2) Global Ozone Monitoring Experiment (GOME); Envisat SCanning Imaging Absorption spectroMeter for Atmospheric CHartographY (SCIAMACHY); Aura OMI; and EUMETSAT GOME-2) make it possible to estimate long-term trends of NO_2 and SO_2 from 1996 to present (e.g., Lu and Streets, 2012; Fioletov et al., 2013).

Relating satellite-derived VCD data trends for a relatively long-lived gas (e.g., CO) to trends in surface pollutant concentrations is more difficult than for a short-lived gas (e.g., SO_2, NO_2). Most of the VCD for a short-lived gas is found near its surface emission sources because its chemical lifetime is short (i.e., hours to about a day depending on meteorological conditions) and its background level is low relative to the level in industrialized areas. On the other hand, a long-lived gas can have a high background concentration relative to that in industrialized areas. The Terra MOPITT product shows that CO decreased by ~1.4%/yr from 2000 to 2012 over the eastern U.S. (Worden et al., 2013), while surface observations show a much stronger response (~5%/yr) over this same period (EPA, 2012). However, He et al. (2013) compared the near-surface MOPITT CO product (Section 5.1.4; Deeter et al., 2012) to EPA AQS observations and found that the estimated decreases were similar (~40%) from 2000 to 2011 in the Baltimore-Washington, DC metropolitan area. As with all data, whether from satellite instruments or surface monitors, the confidence associated with an estimated trend is correlated with the magnitude of the trend relative to data uncertainties (see Section 5.7).

4. Data basics, including processing and visualization resources

NASA satellite data are free and available to everyone, but data access is a commonly reported barrier to data use because of the increasingly large number of data types, metadata, and websites for finding data, all of which can be daunting for the first time user. For beginners, it is recommended to first visit the ARSET website (http://airquality.gsfc.nasa.gov/), which contains

free training materials, and information on instructional webinars and in-person courses; Prados (2012) gives a full description of the ARSET program. Organizations interested in in-person trainings are encouraged to submit an application through the ARSET webpage. ARSET personnel will provide general guidance to end-users on data for specific AQ applications, but they will not provide data analysis upon request. Instead, end-users are encouraged to contact members of AQAST (http://acmg.seas.harvard.edu/aqast/) for assistance.

This section provides the basics of using satellite data for AQ applications, including direction for finding imagery, data maps, data files, and a list of some of the most popular free web-based and downloadable analysis tools (**Table 2**).

4.1 Levels of data and spatial resolution

Satellite data come in various 'Levels' which indicate the degree of processing. Level 0 (L0) data are the raw data obtained from the instrument and are processed to Level 1 (L1). L1 data are produced by applying the instrument pre and post-launch calibrations to produce radiances and then geolocating these data. Level 2 (L2) and Level 3 (L3) data are processed from L1 to a geophysical parameter, such as AOD or NO_2 VCD. The relevant Levels for AQ applications are L2 and L3. The key difference between L2 and L3 is that L2 data are the original geolocated observations and not spatially gridded while the L3 data are mapped to a regular spatial grid (e.g., 0.25° latitude x 0.25° longitude), and averaged over time, such as a day or month. **Figure 7** shows an example of a Terra MODIS L2 image of AOD. The spatial resolutions of L2 data vary widely between instruments (e.g., 250 m x 250 m, fractions of degrees latitude and longitude). L3 data generally have lower spatial and temporal resolutions than L2 data, but they have the advantage of being easier to read, visualize, and analyze. L3 data may be adequate for most regional AQ applications, but the majority of end-users find that L2 data are better suited for examining point sources or urban pollution.

4.2 Temporal resolution and latency

The temporal resolution of satellite data is determined by many factors, including the satellite type (e.g., polar-orbiting vs. geostationary; Section 5.4), the orbital swath width of the instrument (i.e., the width of the "stripe" of the Earth's surface observed as a satellite overpasses), and the degree of snow cover and cloud cover (e.g., **Figure 6b**). Most NASA data are from instruments

on polar-orbiting satellites (e.g., Terra, Aqua, and Aura) that have 90-minute sequential orbits, thus achieving global coverage in a day or two. That is, the data are collected daily at approximately the same local time (±45 minutes) at every location of the globe. For instance, the Aura satellite overpasses any given location once in early afternoon local time while the Terra satellite overpasses a location once in mid-morning. L2 data have a time stamp in the data files associated with each ground pixel. L3 data, which are processed to a specific horizontal grid and are an aggregate of the L2 data over time, do not have a time stamp associated with each observation.

Latency refers to the time after an observation is made until the data become publicly available through a NASA web portal. An increasingly large number of "near-real-time" products become available via NASA websites (**Table 2**) within a few hours of the instrument's data collection. The data are processed quickly to obtain L2 and L3 products that are intended for operational use, such as AQ forecasting or disaster management. While near-real-time products are often high quality, the L3 data are carefully reprocessed later, so that the near-real-time and final products may not be identical.

4.3 Access to data files

Official NASA products are managed by NASA's Earth Observing System Data and Information System (EOSDIS) and its twelve data centers, which archive data from the beginning of each mission, thus enabling retrospective studies and analysis. EOSDIS has several search engine tools, such as Reverb, which allows end-users to search available data files by instrument, sensor, and pollutant type. Files can also be temporally and spatially sub-setted so that it is not necessary to download entire global files, which can be large. Gas and aerosol products can be found at the Goddard Earth Sciences Data and Information Services Center (GES DISC) and at the Langley Research Center Atmospheric Science Data Center (LaRC ASDC). Near-real-time products can be accessed via NASA's Land Atmosphere Near real-time Capability for EOS (LANCE) (**Figure 8**).

4.4 Visualization and analysis tools

The most commonly used tools for the visualization and analysis of NASA satellite data are described in this section and **Table 2**. Most NASA websites provide imagery in commonly-used

file formats, including gif, png, kml or kmz (for Google Earth visualization), web map service (wms), and GIS. For a comprehensive list of web tools please visit the ARSET website, which provides tables of available web tools for accessing satellite data for 1) specific pollutants, such as NO_2, CO or aerosols, 2) fire and smoke products, and 3) true color imagery. Many NASA products are available from multiple web tools. To help end-users find the most suitable tool for their needs, the ARSET tables also contain information on the characteristics of the satellite data in each web tool, such as spatial and temporal resolution, data file formats and level of processing (e.g., L2, L3).

4.4.1 Gas and aerosol products

Maps and basic customized analysis of satellite and ground-based geophysical parameters, such as pollutant VCDs or aerosol extinction profiles, can be obtained from a variety of NASA websites. These web-based tools enable end-users to easily make images online by searching and selecting the needed parameters and specifying the dates and geographical area of interest. Three of the most popular tools are Worldview, Giovanni, and LAADS Web. The LANCE interface (**Figure 8**) provides access to Worldview and is NASA's main tool for visualization and download of near-real-time data and imagery, including for gases, aerosols, fire locations and true color imagery. Giovanni allows the user to perform simple analysis, such as time series and multi-day area-averaged image maps, without the need to download software (Prados et al., 2010). Data files and images of aerosol and gas observations are available under the "Air Quality" or "Atmospheric Portals." LAADS Web provides easy access to L1 data from MODIS and VIIRS.

There are also multiple stand-alone image visualization packages for download, many at no cost. They range from simple visualization tools, such as *Panoply* from the NASA Goddard Institute of Space Studies, to more sophisticated packages, such as *HDF Look*, that provide both data visualization and analysis capabilities. ARSET trainings provide guidance on the use of all these tools, and training modules can be found on the ARSET website under the "tools" section.

Other federal agencies provide visualization and analysis capabilities of NASA satellite products. The Infusing Satellite Data into Environmental Applications (IDEA) web tool is supported by NOAA National Environmental Satellite, Data, and Information Service (NESDIS) and provides near-real-time access to MODIS and GOES aerosol products and meteorological

information. IDEA also provides maps and time series of both $PM_{2.5}$ measured by surface monitors and $PM_{2.5}$ derived from satellite AOD data to facilitate comparisons between satellite and surface observations. The $PM_{2.5}$ maps also include forward trajectories at multiple pressure levels initialized in regions of enhanced AOD. The Remote Sensing Information Gateway (RSIG) tool at the EPA is designed to facilitate comparisons between CMAQ model output and NASA and NOAA satellite data.

4.4.2 Near-real-time true color imagery and fire products

True color imagery provides qualitative information about AQ that can be very valuable in representing the "big picture" of what is occurring regionally, such as for determining the location of forest fire smoke plumes and smoke plume extent (e.g., **Figure 3**). This type of imagery closely resembles what the naked eye sees. Current fire locations and burned area products from the MODIS instrument are available from the LANCE FIRMS website. The NOAA Hazard Mapping System Fire and Smoke Product (HMS) provides fire locations from MODIS and smoke plume extent from GOES and MODIS, and is used frequently by first responders, forecasters, and in exceptional event demonstration packages (Section 2.3). For a comprehensive list of websites that provide true color imagery, including near-real-time imagery, visit the ARSET website under the "Satellite Imagery" section.

4.4.3 Exceptional Event Decision Support System (EE DSS)

The Washington University in St. Louis has developed an Exceptional Event Decision Support System (EE DSS) that facilitates the analysis of both surface and satellite data for exceptional event submissions. EE DSS is hosted by DataFed, which provides a wealth of satellite and surface AQ data from NOAA, NASA, EPA, and other entities. EE DSS features distinct data analysis portals for the various criteria required by EPA to justify data exclusions due to an exceptional event. Time series of ozone, PM_{10} and $PM_{2.5}$ from surface monitors can be easily plotted along with the relevant NAAQS to help determine whether the measured concentration is above the NAAQS threshold and whether it is beyond typical levels. There is also a console that provides MODIS true color imagery, AOD and NO_2 data, and meteorological data hosted by DataFed, to help regulators seeking to analyze a causal relationship between the measurement under consideration and the exceptional event.

5. Straight answers to frequently-asked questions (FAQs)

People involved in ARSET and AQAST are asked many questions concerning the use of satellite data for AQ applications. Here are answers to some of the most frequently-asked questions.

5.1 Can satellites measure "nose-level" concentrations?

The short answer is "no" because the majority of satellite instruments that measure pollutants of interest to the AQ community are downward-looking, providing limited information on the vertical structure of the pollutant in the atmosphere. Satellite instruments that measure ozone, NO_2, HCHO and SO_2 only detect the number of molecules between the instrument and the Earth's surface. (There are efforts to improve this situation (e.g., Section 5.1.1).) As mentioned in Section 2.3, this quantity is typically referred to as a "vertical column density" (VCD) in units of molecules per unit area of the Earth's surface. Nevertheless, these data are highly useful in many AQ applications, including for inferring "nose-level" concentrations as discussed in this section. For aerosols, satellite instruments observe AOD, which is a measure of the integrated extinction by aerosols of light passing through the entire atmospheric column from the surface of the Earth to the satellite instrument. Surface $PM_{2.5}$ may be inferred from AOD data in many instances (Section 5.1.6). For more in-depth discussions of issues associated with detecting surface concentrations from space, beyond what is presented in this section, the reader is referred to Fishman et al. (2008), Martin (2008), and Hoff and Christopher (2009).

5.1.1 Are there satellite data for surface ozone?

The development of a surface ozone product is fraught with many obstacles, so that such a product is not currently feasible. First, the portion of the ozone VCD that is in the troposphere is about 10 times less than the amount in the stratosphere (e.g., "ozone layer"), making it very difficult for satellite instruments to discriminate the stratospheric and tropospheric amounts. There are several methods to separate the portion of ozone found in the stratosphere from that found below the stratosphere (e.g., Fishman et al., 2003). However, the relation is complicated for the tropospheric, including lower tropospheric, ozone VCDs and near-surface ozone (e.g., de Laat et al., 2005; Chatflield and Esswein, 2012). An AQ model is required to properly interpret

the tropospheric ozone VCD from satellite data. However, Flynn et al. (2014) suggest that ozone partial column densities from future satellite instruments with sufficient sensitivity to the lower troposphere can be meaningful for surface AQ analysis. Second, ultraviolet (UV) wavelengths of light, which are used for detecting and measuring ozone, are strongly obscured by atmospheric scattering, which limits their ability to reach the Earth's surface. Infrared (IR) wavelengths can also be used for inferring ozone in the troposphere, but the products are sensitive to the input parameters used to create them (see Section 5.2.1). Research is ongoing that could enable measurements of boundary layer ozone, which is based on using the combination of UV and IR wavelengths (e.g., Worden et al., 2007; Zoogman et al., 2011). Existing instruments, such as OMI, use only UV and visible wavelengths. Therefore, it is problematic to quantify the amount that is near the surface, including at "nose-level". Nevertheless, the tropospheric ozone VCD sometimes correlates well with surface data, including in urban areas (Kar et al., 2010).

There are satellite data that give information near the surface on ozone's chemical precursors (i.e., NO_x (Section 5.1.2) and VOCs (Section 5.1.3)), including emission estimates (Section 3.1; Streets et al., 2013). Together, NO_2 and formaldehyde VCD data can be used to infer the chemical sensitivity (i.e., "VOC-limited" versus "NO_x-limited" regimes) of ozone production near the surface. Sillman (1995) used correlations between surface observations of various pollutants (e.g., formaldehyde and total reactive nitrogen (NO_y)) to determine this chemical sensitivity. Martin et al. (2004) applied the technique of Sillman (1995) to satellite observations, using the ratio of the VCDs for formaldehyde and NO_2 from GOME data. Duncan et al. (2010) expanded on the work of Martin et al. (2004) with OMI data, finding that the majority of the U.S. is now in the NO_x-limited regime due to recent reductions of the emissions of NO_x (Section 3.2). Please refer to Duncan et al. (2010) for more details on using satellite data as an AQ indicator. New satellite instruments, with higher spatial resolution, that observe both NO_2 and formaldehyde are currently being developed (Section 5.11.1).

5.1.2 Are there satellite data for surface NO_2?

While it is not feasible to measure surface NO with current instruments (e.g., Bovensmann et al., 1999), surface NO_2 is readily detected. The NO_2 VCD serves as an effective proxy for NO_x and correlates well with surface levels of NO_2 in industrialized regions (e.g., Leue et al., 2001; Velders et al., 2001). Most of the NO_2 VCD is found near its surface emission sources because

its chemical lifetime is short (i.e., hours to about a day depending on meteorological conditions) and its background level is low relative to the level in industrialized areas. Like ozone, there is a significant contribution to the NO_2 VCD from the stratosphere, but it can be subtracted (e.g., Bucsela et al. (2013) and references therein). Even if the stratospheric portion is not removed, the local gradients in the VCD are associated with gradients near the surface in polluted regions as the distributions of NO_2 in the stratosphere are rather uniform. This subtraction is already done in the L2 and L3 OMI NO_2 products (Section 4.1). Airborne measurements over polluted areas suggest that the portion of the NO_2 column in the boundary layer could be over 75% of the tropospheric VCD over land (Martin et al, 2004; Bucsela et al, 2008). Ordonez et al (2006) demonstrated a strong correlation between the tropospheric NO_2 VCD and NO_2 observations from the EPA AQS. Lamsal et al (2008, 2010) developed a method for estimating surface NO_2 from the OMI NO_2 product, finding that their OMI-derived surface NO_2 concentrations were well correlated with surface AQS measurements, both temporally (r = 0.3-0.8) and spatially (r = 0.76). Knepp et al. (2013) found that VCD data from a ground-based suntracking spectrometer system, which is similar to OMI, compared well to "nose-level" NO_2 data collected nearby when the daily cycle of boundary layer mixing was taken into account.

5.1.3 Are there satellite data for surface VOCs?

There is a myriad of VOC compounds that contribute to ozone formation, but only a few can be detected from space (e.g., methanol, formaldehyde, glyoxal, and peroxyacetyl nitrate (PAN)). Formaldehyde can serve as a proxy for total VOC chemical reactivity with the hydroxyl radical (OH; e.g., Chameides et al., 1992) as most VOCs react with OH and are, subsequently, oxidized to formaldehyde. It has been shown that the variability in the distribution of formaldehyde is highly correlated with isoprene (Palmer et al., 2003, 2006; Millet et al., 2008), a VOC emitted by trees that is known to play an important part in the formation of ozone in the eastern U.S. (Chameides et al., 1988). The strong temperature-dependence of isoprene emissions has been inferred from satellite data (Abbot et al., 2003; Palmer et al., 2006). Like NO_2, most of the gradient in the formaldehyde VCD data is correlated with the distribution of surface sources as its chemical lifetime is relatively short. Formaldehyde data have a large uncertainty associated with them, so care should be taken when using the data (see Section 5.7).

5.1.4 Are there data for surface CO?

There are several instruments that measure infrared (IR) wavelengths of light to infer CO concentrations. Instruments that observe thermal-infrared (TIR) wavelengths can measure CO in the free troposphere, though the vertical resolution is rather poor (e.g., only one or two levels). Data from these instruments have been shown to be useful, for instance, in tracking the long-range transport of pollution, such as from wildfires, but they do not provide information on "nose-level" CO. Instruments that observe near-infrared (NIR) wavelengths give information on CO VCD, which can be used to infer surface emissions and where high levels of CO occur. Currently, Terra MOPITT, was launched in 1999, measures near-surface CO (surface - 900 mb). It observes both TIR and NIR wavelengths and the recent algorithms are making use of this complementary information to infer CO near the surface (Deeter et al., 2012). There are several limitations of this product: only land surfaces during daytime have information in the NIR and the measurement sensitivity to near surface CO has large variability over different surface types, so end-users are urged to understand the limitations of the data for their particular application.

5.1.5 Are there data for surface SO_2?

Most of the SO_2 VCD is near surface sources as its lifetime is short. SO_2 data have proven quite useful for some AQ applications, such as observing changes in pollutant levels from large point sources (e.g., **Figure 5**; Fioletov et al., 2011), but it is not currently useful for analyzing day-to-day variations, such as during an AQ event; SO_2 data need to be carefully processed and interpreted (see Section 5.8). Research is ongoing to improve the data and there have been recent important advances (e.g., Li et al., 2013).

5.1.6 Are there data for surface $PM_{2.5}$?

Satellite instruments do not measure $PM_{2.5}$ directly, but do observe AOD, which is a measure of the integrated extinction by aerosols of light passing through the entire atmospheric column from the surface of the Earth to the satellite instrument. If $PM_{2.5}$ is well mixed in the boundary layer and skies are free of clouds, the AOD-$PM_{2.5}$ relationship can be expressed as:

$$AOD = PM_{2.5} \times H \times f(RH) \times \frac{3Q_{ext,dry}}{4\rho r_{eff}} \quad (1)$$

where H is the boundary layer height, f(RH) is the ratio of ambient and dry extinction coefficients, ρ is the aerosol mass density, $Q_{ext,dry}$ is the Mie extinction efficiency, and r_{eff} is the particle effective radius (Hoff and Christopher, 2009). The conversion of AOD data to surface $PM_{2.5}$ data is complicated as it requires knowledge of various factors that influence AOD, such as relative humidity (e.g., Case Example #1; **Figure 2**), aerosol composition (e.g., soot, dust), and the altitude of the aerosol layer (e.g., Wang and Christopher, 2003; Engel-Cox et al., 2004; Zhang et al., 2009; Crumeyrolle et al., 2013). Appendix A contains a discussion of satellite prediction of surface $PM_{2.5}$ levels.

5.2 Why are there multiple products for the same species?

5.2.1 Why are there multiple products for some species from the same instrument and which should I use for my application?

Satellite instruments measure the scattering or emission of electromagnetic radiation by the atmosphere, not atmospheric quantities of pollutants (Section 5.5). The conversion of electromagnetic radiation to an atmospheric quantity, which is referred to as a "retrieval algorithm", is a complicated and multi-step process (e.g., Sections 5.5 and 5.6). Often there are a number of ways posed and tested by research groups to derive this atmospheric quantity. Consequently, multiple products can exist for the same pollutant from the same instrument. In addition, the refinement of a specific retrieval algorithm may occur over many years, leading to multiple versions (presumably with incremental improvements) of a given product from the same research group. For example, NO_2 VCD data have proven highly valuable for AQ applications as discussed in Section 3. There are two main products that are available for OMI on the NASA Aura satellite. The early releases of the products, one from NASA and the other from the Royal Netherlands Research Institute (KNMI), often disagreed by up to a factor of two for some regions (e.g., Lamsal et al., 2010). However, the current, refined retrieval algorithms of both research groups, though different in their approaches, now produce very similar atmospheric quantities (e.g., Bucsela et al., 2013). The refinement of these algorithms will likely continue for some time as researchers strive to improve their products.

End-users, who are not experts in retrieval algorithms, do not always know which product is best suited for their applications. Ultimately, the onus is on the end-user to understand the

strengths and limitations of a particular product so as to decide which one is most appropriate for the particular AQ application and to properly interpret the data. There are now a number of helpful resources, including the AQAST and ARSET programs, at the disposal of the end-user to simplify this task (Section 4).

5.2.2 Why are there multiple instruments that measure the same quantity?

Some atmospheric quantities are measured by several satellite instruments. This occurs for a variety of reasons. First, individual countries, including the U.S., the European Space Agency (ESA), and Japan, support their own satellite programs. Second, some instruments provide data for a particular area (e.g., North America) or a particular time of day. As an example, the GOES satellite observes AOD levels over North America in a geostationary orbit, while the MODIS instruments on the Terra and Aqua satellites provide global coverage at approximately 10 am and 2 pm local times, respectively. Third, replacement instruments are generally launched before the end of life of aging instruments so that there is a period of overlap when both instruments are collecting data. This is important for the creation of long-term data records from multiple instruments. For instance, long term records of NO_2 and SO_2 could be created from data collected by the GOME (1995-2003), SCIAMACHY (2002-2012), OMI (2004-present), and GOME-2 (2006-present) instruments, though one would need to consider variations in spatial coverage, overpass time, and horizontal resolution of each of the instruments (e.g., Lu and Streets, 2012; Fioletov et al., 2013). Finally, in some cases, instruments designed to measure a particular pollutant or set of pollutants will have sufficient capability to observe other pollutants that the instrument was not originally designed to measure.

5.3 Are there data with finer spatial resolution?

As discussed in Section 4.1, the spatial resolutions of products vary widely, depending on the instrument and the level of data processing. Ultimately, the data with highest spatial resolution for a specific product is a tradeoff between the sensitivity and pixel size of the instrument. As with a photo from a common digital camera, the image produced from a satellite instrument is composed of many pixels. The spatial area of the Earth's surface observed by a pixel is often referred to as a pixel's "footprint". The footprints of individual pixels on the same instrument can vary, particularly if the instrument scans the atmosphere from either side of the orbital track

where the pixel size increases as the viewing angle increases. The pixel that views the atmosphere directly below it (i.e., perpendicular to the Earth's surface) is referred to as the "nadir" pixel and has a footprint of, for instance, 13 x 24 km^2 in the case of OMI and 10 x 10 km^2 or 3 x 3 km^2 for MODIS. For OMI, the largest footprint is ~13 x ~150 km^2 (Levelt et al., 2006). All the pixels together observe an area 2600 km wide, which is referred to as the "field of regard", with each overpass.

The advantage of a wide field of regard is that it allows for daily global coverage of the entire Earth's surface. The disadvantage is that the footprints of many pixels are too large for AQ applications. Advanced versions of OMI are under development which will have smaller pixel sizes (see Section 5.11.1). Statistical methods can be used to decrease pixel size, such as the technique of "oversampling" the data (e.g., de Foy et al., 2009; Fioletov et al., 2011; Streets et al., 2013), but this requires averaging data over time and losing some temporal resolution to achieve statistical significance (see Section 5.7) of the data on the finer horizontal grid.

5.4 Are there data that span the entire day?

For AQ applications, an instrument on a satellite in geostationary (or geosynchronous) orbit is ideal as this allows for continuous observations of the same region (e.g., the U.S.); the satellite's orbital period matches the Earth's rotational period, so the satellite appears to be motionless to an observer on the Earth's surface. The NOAA GOES series is an example of geostationary satellites and the current GASP product from the GOES-West and GOES-East instruments provides AOD at 30 minute intervals throughout the day. NASA is actively planning a geostationary satellite, called Tropospheric Emissions: Monitoring of Pollution (TEMPO), with instruments that will measure pollutants relevant for AQ applications and NOAA will be launching the GOES-R series beginning in 2016, which will also provide aerosol products (Section 5.11).

Currently, almost all instruments that provide information on pollutants, such as AOD, NO_2, SO_2, and formaldehyde, are onboard polar-orbiting satellites, which overpass a given location in the U.S. approximately once a day during daylight hours. Because polar-orbiting satellites have different overpass times, for certain pollutants it is possible to obtain a limited amount of information on their daily variability. For instance, data are collected from OMI on the Aura satellite, which has an early afternoon overpass, and from GOME-2 on the EUMETSAT Metop

satellite, which has a morning overpass. In addition, Terra MODIS and Aqua MODIS have 10:30 am and 1:30 pm overpasses, respectively. However, in multi-instrument analysis it is important to account for differences in the capabilities, biases and other characteristics of the individual instruments (e.g., Boersma et al., 2008; Fioletov et al., 2013).

5.5 How does a satellite instrument measure gases and aerosols?

Most satellite instruments that collect data relevant for AQ applications are "passive". ("Active" instruments, such as lidars or radars, send a signal and detect the portion of the signal that returns.) Passive instruments detect electromagnetic radiation from the Sun that is absorbed and reemitted, reflected, and scattered by the Earth and atmosphere. The incoming radiation passes through a spectrometer, a device that measures energy intensity as a function of wavelength, to create a spectrum of wavelengths that are then detected. When individual photons strike the instrument's detector, the energy is converted into electrons as a way of measuring the amount of incoming energy at various wavelengths. The infrared (IR), visible, and ultraviolet (UV) regions of the electromagnetic spectrum contain the most useful wavelengths for observing pollutants relevant for AQ applications as these gases and aerosols absorb IR wavelengths (e.g., water vapor) or scatter visible and UV wavelengths (e.g., dust, NO_2).

5.6 How does one quantify the amount of a pollutant in the atmosphere from satellite data?

Each pollutant absorbs and/or reflects specific wavelengths throughout the electromagnetic spectrum. This "spectral signature" is unique to that pollutant, like a fingerprint is unique to each human. (The reader is directed to Figure 1 of Martin (2008) for an illustration of a spectral signature.) For some pollutants, the unique signature is readily apparent, but for others, the signature overlaps with the signatures of other gases, such as water vapor and ozone in the IR wavelength range (Section 5.7). The magnitude of the quantity of a certain pollutant in the atmosphere can be inferred by comparing the spectral signature recorded by the satellite instrument to a reference signature measured in a lab using a known quantity of the pollutant. In practice, this requires a complicated model of radiative transfer (i.e., the propagation of electromagnetic energy through the Earth's atmosphere) to interpret what is measured by the satellite instrument. The model accounts for the absorption, emission, and scattering of light by

clouds, the Earth's surface, aerosols , and all gases, including the pollutant of interest, as it passes through the Earth's atmosphere to the satellite. Hoff and Christopher (2009) give more details on the equations used in radiative transfer models.

5.7 Why do some products have higher uncertainties than others?

For each satellite product, there is an associated uncertainty which includes bias and precision errors. The overall uncertainty is a combination of uncertainties from a number of sources, such as those associated with the instrument and those introduced during the creation of the product (e.g., Kahn, 2012; Bucsela et al., 2013). For a discussion of the uncertainty, the end-user should consult the documentation that is provided for each product.

Spectral uncertainties: Some pollutants are easier to measure because their spectral signatures are stronger and/or distinct, while others are more difficult, particularly if the spectral signatures overlap with other gases. For example, of the OMI NO_2, SO_2, and formaldehyde products, the overall uncertainty is lowest for the NO_2 product as NO_2 has strong and distinct spectral structure at wavelengths where it is the dominant absorber. That is, it is relatively easy to remove the effects of other species (e.g., ozone, water vapor, etc.) that absorb in the same spectral region. For formaldehyde and SO_2, ozone absorption dominates at wavelengths used in their retrievals. The SO_2 absorption is particularly weak as compared to ozone's absorption.

Uncertainties associated with the creation of VCDs: The "slant" column density (SCD) observed by the satellite is converted to a more useful "vertical" column density (VCD) of a pollutant, which is perpendicular to the Earth's surface (e.g., L2 and L3 data; Section 4.1). This conversion process, which is described in Palmer et al. (2001), is required so that the data may be presented in easy to understand geographic maps. There are multiple uncertainties introduced into a product during this multi-step process (e.g., Leue et al., 2001; Bucsela et al., 2013), which may have implications for a specific AQ application. For instance, Case Examples #1 (Section 2.1) and 2 (Section 2.3) illustrate the utility of true color images and AOD for tracking aerosol pollution, but satellite data for gases (e.g., CO and NO_2) from wildfires require special treatment to properly estimate the VCDs. During the production of a gas product, it is necessary to 1) account for the presence of aerosols, which absorb and scatter light and can interfere with the detection of a gas, and 2) assume an "initial guess" of the atmospheric vertical profile of the concentration of the gas (see Appendix B). Oftentimes, an AQ model is used to estimate the

aerosol loading and the vertical profile for typical conditions (i.e., when there is not a wildfire). However, a fire can cause the aerosol loading and the vertical profile of a gas to be dramatically different as compared to typical conditions. While the influence of wildfires is not routinely accounted for, or only partially accounted for, in the generation of many gas products, it should be to properly estimate the column density of the gas. Otherwise, the gas products are simply qualitative at best for this application.

Research is ongoing to reduce uncertainties, which leads to multiple versions of some gas and aerosol products as incremental improvements are made (Section 5.2.1). Because of these uncertainties and assumptions made in the retrieval algorithms, we use the term "product" when discussing specific datasets in this article, but use "data" when speaking generically about satellite data.

5.8 How do I know if my data are statistically significant and accurate?

As with all data, including from surface networks, a statistical analysis is required so that the end-user does not draw an erroneous conclusion - a common mistake that should be avoided. Here we discuss briefly random and systematic errors.

Random Error: If the error for a given product is random, it will cancel in the average over space and/or time. That is, individual observations may be imprecise, but their average is precise. Therefore, one must consider the time-averaging interval used in a trend analysis, for instance. The overall confidence that the average is statistically significant increases with the square root of the number of individual overpasses (N) included in the average. However, the N required for statistical significance increases as uncertainty increases (i.e., as the precision decreases), so it can vary significantly from pollutant to pollutant. As a general rule of thumb, one should average data on the order of weeks for tropospheric NO_2, six weeks or more for formaldehyde, and a year or more for SO_2, depending on the degree of concomitant spatial averaging and overall concentration of the pollutant. For example, Duncan et al. (2013) used the OMI NO_2 product as a proxy for the month-to-month changes in NO_x emissions from power plants in the U.S. For their analysis, they required a fine horizontal resolution (0.1° latitude x 0.1° longitude) to isolate the signal of the power plant. However, they found that N was often too low for statistical significance at these horizontal and temporal resolutions, particularly in winter in regions with persistent snow and/or cloud cover (e.g., **Figure 6b**).

The treatment of errors in AOD is dependent on the specific application. When converting AOD to $PM_{2.5}$, the random AOD retrieval error is often carried through the statistical model (Appendix A) into the $PM_{2.5}$ estimates. Most advanced models developed in the U.S. can estimate daily $PM_{2.5}$ concentrations. These estimates are then averaged spatially (e.g., from the modeling grid cells to a county in order to be linked to population and disease characteristics) and/or temporally (e.g., from daily to weekly, monthly, or a longer period for trend analysis). At this stage, the random error in individual $PM_{2.5}$ predictions is reduced through averaging. For applications requiring daily $PM_{2.5}$ estimates at the model's highest spatial resolution (e.g., air pollution episode analysis), such errors can be quantified at the level of the dataset or individual estimates with standard metrics such as root mean square error, relative error and techniques such as cross-validation. The end-user then must decide whether the model performance is sufficient before drawing conclusions based on the mean $PM_{2.5}$ estimates.

In polluted regions, pollutant levels for AOD and NO_2 may be high enough that one can use the data to analyze an individual AQ episode, which typically lasts only a few days, but a larger N is necessary in less polluted regions. It is not advised to put much faith in the VCDs for formaldehyde and SO_2 on the time scales of an AQ episode, even if they appear to be credible; the VCDs will be semi-quantitative, at best, and not statistically significant.

Systematic Error: In addition to random error, a systematic error causes data to be biased relative to other "ground truth" observations, such as those taken by instruments on aircraft or in surface networks. That is, a systematic error reduces the accuracy of the data. A bias may be a function of, for example, region and season. As with a random error, a systematic error may be introduced during the conversion of the observed SCD to a VCD, but it cannot be removed by spatial or temporal averaging. Biases may also be associated with instrument artifacts. As an example, a problem that is unique to OMI is that orbital "stripes" appear in horizontal maps of the OMI products (e.g., Bucsela et al., 2013). It is worth noting that even a biased product may be precise. The issue of bias is particularly important for SO_2. For instance, Fioletov et al. (2011) used the OMI SO_2 product to estimate the change over time in SO_2 emissions from power plants (**Figure 5**). They found that the data had large-scale, spatial patterns over the U.S. They were able to account for the spatial bias by averaging SO_2 data within a 300 km radius of a power plant and then subtracting this regional mean from the SO_2 data in the power plant plume. An example for aerosols is that the Multi-angle Imaging SpectroRadiometer (MISR) tends to

overestimate AOD at low levels (Kahn et al., 2010) and underestimate AOD at extremely high levels rarely seen in developed countries (Jiang et al., 2007). As a result, using MISR data to estimate $PM_{2.5}$ would potentially lead to an overestimate in a clean environment and an underestimate in a severe pollution episode. The latest MODIS 3 x 3 km^2 AOD product has been shown to have a positive bias in urban areas (Munchak et al., 2013). More importantly, the systematic error of satellite AOD is often proportional to the AOD value itself and can vary with weather conditions (e.g., proximity to clouds) and surface types (e.g., impervious surfaces or snow cover). In the setting of a quantitative analysis, the user is advised to contact the satellite instrument teams early for appropriate procedures regarding systematic error correction.

5.9 What is the best way to evaluate model output with satellite data?

Appendix B provides a brief description of the steps required to perform an "apples-to-apples" comparison of model output and satellite VCD data using the OMI NO_2 product as an example. Since the steps presented in Appendix B are not universally applicable to all satellite products, the end-user is encouraged to contact the product developers for guidance.

If variables called "scattering weights" or "averaging kernels" are provided in the satellite data file, the end-user should perform the additional step of applying them to a model's vertical concentration profile for a proper comparison. Scattering weights are associated with column density data and averaging kernels are generally associated with data of vertical profiles. They arise from the fact that satellite instruments are more sensitive to the presence of gases at higher altitudes. They are critical for interpreting the information content in the product, particularly for satellite instruments that measure a pollutant using IR wavelengths, such as MOPITT. As a word of caution, the phrase "averaging kernel" is often defined differently for different products.

In addition, a proper comparison of model output to observational data, whether from satellites or surface monitors, requires the end-user to become familiar with the strengths and limitations of the data for evaluating a model's pollutant distributions. It is important to understand the relationship between, for example, surface NO_2 (ppbv) and NO_2 VCD (molecules/cm^2) as discussed in Section 5.1.2 and AOD (unitless) and $PM_{2.5}$ ($\mu g/m^3$) as discussed in Section 5.1.6.

5.10 Is it true that satellite data will replace the need for surface observational networks?

No. There remain fundamental limitations to measuring surface pollution from space as discussed above (e.g., Sections 5.1 and 5.7) so that satellite data will not supplant the need for surface networks. As discussed in Section 2, spatial coverage is the strength of satellite data over surface observational networks. That is, satellite data provide complementary information to measurements collected at the surface by "filling the gaps" between monitors. Scheffe et al. (2012) argue for better integration of the existing surface network of observations with alternative observational platforms, including satellite-based ones.

5.11 What new and improved satellite missions are being built?

There is currently no satellite instrument in orbit that is optimized for AQ applications and the few upcoming instruments discussed in this section, though improved as compared to current instruments for AQ applications, will not supplant the need for surface observations (Section 5.10). For a variety of reasons, including the prohibitive costs of some missions and the risk of a satellite failing to reach orbit, NASA is exploring ways to design smaller and more cost-effective orbital and suborbital missions through its Earth Venture program. (Both the TEMPO (Hilsenrath and Chance, 2013) satellite mission, discussed in Section 5.11.1, and the DISCOVER-AQ (Section 2.1) suborbital mission are examples of NASA Earth Venture missions.) Therefore, there is the opportunity for funding innovative and cost-effective ways to collect data on air pollution, such as by placing smaller versions of satellite instruments on drones or dirigibles that could hover over urban areas on days with poor AQ.

5.11.1 What new and improved satellite missions are being built for gases?

For gas pollutants (e.g., NO_2, SO_2), two satellites, one from NASA and the other from the European Space Agency (ESA), will have sensors similar to Aura OMI and are currently under construction with tentative launch dates within the next five years. Both missions promise enhanced observational capabilities over those of OMI, which is important given the recent, substantial decreases in SO_2 and NO_2 levels in the U.S. (e.g., **Figures 4-5**). The TEMPO (Hilsenrath and Chance, 2013) instrument will be in geostationary orbit over North America, collecting hourly data throughout the day as opposed to one overpass per day as with OMI. The hourly observations will improve precision of the measurement and enable a better horizontal

resolution (2 x 4.5 km^2) than OMI's. The planned launch is 2018 or 2019. The ESA Tropospheric Ozone Monitoring Instrument (TROPOMI) is an OMI follow-on instrument with finer horizontal resolution (i.e., 7 x 7 km^2) than OMI and will fly on the polar-orbiting Sentinel-5 Precursor satellite. The planned launch date is 2015. Currently, there are no planned instruments by NASA to replace the Terra MOPITT instrument, which provides CO VCD data that have proven useful for tracking pollution plumes and estimating source emissions (e.g., Streets et al., 2013). TROPOMI will include instrument capabilities similar to SCIAMACHY, which flew on ESA's defunct Envisat satellite. Therefore, it will provide CO and methane VCDs, but it will not provide information on CO near the surface as is the case with MOPITT.

5.11.2 What new and improved satellite missions are being built for aerosols?

There are few upcoming missions being built that are relevant for estimating surface aerosols. Several instruments currently provide AOD, such as the two MODIS sensors on the NASA Terra and Aqua satellites, and on NOAA GOES satellites. Similar to instruments that measure gases, many now in orbit are past their design lives. The recently launched NPP VIIRS (e.g., **Figure 2a)** also provides AOD, and the Advanced Baseline Imager (ABI) on the NOAA GOES-R satellite, with a planned 2016 launch, will likely continue the record of AOD. In addition, the geostationary satellite, TEMPO, should give more accurate information on the short-term evolution of aerosol plumes than the GASP product, which is sometimes used in exceptional event demonstrations for wildfires (Section 2.3).

Additional information on aerosols is desired to enable use of satellite data for decision support. First, the importance of the distribution of aerosol in the vertical is illustrated in Case Example #1 (Section 2.1)). Information on the vertical distribution is currently collected for near-source aerosol plumes by the MISR and downwind by the CALIPSO instruments, but there are no follow-on missions currently being built to provide this information. Second, another important piece of information is aerosol type, which MISR has the some capability to distinguish (Kahn et al., 2010; e.g., Patadia et al., 2013). Aerosol type data are also available from CALIPSO (nadir view only) and from the surface-based AErosol RObotic NETwork (AERONET; Holben et al., 1998, 2001). However, limitations of these data include spatial and temporal coverage. Third, particle size distribution is another desired piece of information. It is also available from AERONET, qualitatively from MISR, and over water from MODIS. While

not in the “build-phase”, a NASA satellite called Aerosol/Cloud/Ecosystems (ACE) has been proposed and it would provide more comprehensive measurements of aerosols to distinguish aerosol types and associated optical properties, such as size distribution. Fourth, the retrieval algorithms used to create aerosol products are not optimized for AQ applications. For instance, information is needed on land surface properties in urban areas, such as reflectivity, at high spatial resolution to capture the gradients in aerosol distributions (e.g., Lyapustin et al., 2011a,b; Chudnovsky et al., 2013a,b).

6. Summary and charge to the applied AQ community

Many AQ managers are not yet taking full advantage of satellite data for their applications because of the challenges associated with accessing, processing, and properly interpreting NASA’s observational data. That is, a degree of technical skill is required on the part of the data end-user, which is often problematic for organizations with limited resources. Therefore, NASA initiated two complementary programs, AQAST and ARSET, to facilitate the use of satellite data by the AQ community. The overall goal of this review article, an AQAST-ARSET joint effort, is to acquaint the end-user with some background information on satellite capabilities for measuring pollutants, discuss resources available to the end-user, and provide answers to common questions in plain language. Though current satellite products cannot provide “nose-level” concentrations of pollutants, we highlight the value of the satellite data for AQ applications, including estimating emissions, tracking pollutant plumes, supporting AQ forecasting activities, providing supporting evidence for “exceptional event” packages to EPA, monitoring regional long-term trends, and evaluating AQ models.

Current NASA satellite instruments, observing strategies, and retrievals are not designed or optimized specifically for U.S. AQ applications nor has the full potential of satellite data for AQ applications been realized. Therefore, we strongly encourage regulatory agencies engaged in decision support and other stakeholders involved in AQ management to work closely with ARSET and AQAST to explore novel applications of the satellite data. ARSET and AQAST can also serve as a conduit of information between decision makers in the field and the scientists who develop the products so that they may be improved and tailored for the specific needs of the AQ community. This feedback is particularly important for future satellite instrument development and mission planning.

Acknowledgments

This work was funded by the NASA Air Quality Applied Sciences Team (AQAST) and the Applied Remote SEnsing Training (ARSET) program, within NASA's Applied Sciences Program. We thank Ginger Butcher, the NASA Aura Mission's education and public outreach lead, for her comments which greatly improved the readability of the article.

References

Abbot, D., Palmer, P., Martin, R., Chance, K., Jacob, D., Guenther, A., 2003. Seasonal and interannual variability of North American isoprene emissions as determined by formaldehyde column measurements from space. Geophys. Res. Lett. 30(17), 1886. doi:10.1029/2003GL017336.

Allen, D., Pickering, K., Pinder, R., Henderson, B., Appel, K., Prados, A., 2012. Impact of lightning-NO on eastern United States photochemistry during the summer of 2006 as determined using the CMAQ model. Atmos. Chem. Phys., 12, 1737-1758, doi:10.5194/acp-12-1737-2012.

Beirle, S., Boersma, K., Platt, U., Lawrence, M., Wagner, T., 2011. Megacity emissions and lifetimes of nitrogen oxides probed from space. Science 333, 1737–1739.

Boersma, K., Jacob, D., Eskes, H., Pinder, R., Wang, J., van der A, R., 2008. Intercomparison of SCIAMACHY and OMI tropospheric NO_2 columns: Observing the diurnal evolution of chemistry and emissions from space, J. Geophys. Res., 113, D16S26. doi:10.1029/2007JD008816.

Bovensmann, H., Burrows, J., Buchwitz, M., Frerick, J., Noël, S., Rozanov, V., Chance, K.V., Goede, A.P.H., 1999. SCIAMACHY: Mission Objectives and Measurement Modes, 56, 2, J. Atmos. Sci., 127-150.

Bucsela, E. J., et al., 2010. Lightning-generated NO_x seen by the Ozone Monitoring Instrument during NASA's Tropical Composition, Cloud and Climate Coupling Experiment (TC4). J. Geophys. Res. 115, D00J10, doi:10.1029/2009JD013118.

Bucsela, E., Krotkov, N., Celarier, E., Lamsal, L., Swartz, W., Bhartia, P., Boersma, K., Veefkind, J., Gleason, J., Pickering, K., 2013. A new algorithm for retrieving vertical column NO_2 from nadir-viewing satellite instruments: Applications to OMI, Atmos. Meas. Tech. 6, 2607-2626, doi:10.5194/amt-6-2607-2013.

Castellanos, P., Boersma, K.F., 2012. Reductions in nitrogen oxides over Europe driven by environmental policy and economic recession. Scientific Reports 2, 265.

Chameides, W., Lindsay, R., Richardson, J., Kiang, C., 1988. The role of biogenic hydrocarbons in urban photochemical smog: Atlanta as a case study. Science 241, 1473-1475.

Chameides, W., Fehsenfeld, F., Rodgers, M., Cardelino, C., Martinez, J., Parrish, D., Lonneman, W., Lawson, D., Rasmussen, R., Zimmerman, P., Greenberg, J., Middleton, P., Wang, T., 1992. Ozone precursor relationships in the ambient atmosphere. J. Geophys. Res. 97, D5, 6037-6055.

Chatfield, R., Esswein, R., 2012. Estimation of surface O_3 from lower-troposphere partial-column information: Vertical correlations and covariances in ozonesonde profiles. Atmos. Environ. 61, 2012, p. 103–113, dx.doi.org/10.1016/j.atmosenv.2012.06.033.

Chudnovsky, A., Kostinski, Lyapustin, A., and Koutrakis, P., 2013a. Spatial scales of pollution from variable resolution satellite imaging. Environmental Pollution, Vol. 172, 2013 (pp. 131-138).

Chudnovsky, A., Tang, C., Lyapustin, A., Wang, Y., Schwartz, J., Koutrakis, P., 2013b. Critical Assessment of High Resolution Aerosol Optical Depth (AOD) Retrievals for fine particulate matter (PM) Predictions, Atmospheric Chemistry and Physics Discussions.

Clarisse, L., Clerbaux, C., Dentener, F., Hurtmans, D., Coheur, P.-F., 2009. Global ammonia distribution derived from infrared satellite observations. Nature Geoscience 2, 479–483.

Crumeyrolle, S., Chen, G., Ziemba, L., Beyersdorf, A., Thornhill, L., Winstead, E., Moore, R., Shook, M., Anderson, B., 2013. Factors that influence surface PM2.5 values inferred from

satellite observations: perspective gained for the Baltimore-Washington Area during DISCOVER-AQ. Atmospheric Chemistry and Physics Discussions, 13, 23421-23459, doi:10.5194/acped-13-23421-2013.

de Ruyter de Wildt, M., Eskes, H., Boersma, K.F., 2012. The global economic cycle and satellite-derived NO_2 trends over shipping lanes. Geophys. Res. Lett. 39, L01802.

Deeter, M., Worden, H., Edwards, D., Gille, J., Andrews, A., 2012. Evaluation of MOPITT retrievals of lower-tropospheric carbon monoxide over the United States. J. Geophys. Res., 117, D13306, doi:10.1029/2012JD017553.

Duncan, B., Yoshida, Y., Olson, J., Sillman, S., Martin, R., Lamsal, L., Hu, Y., Pickering, K., Retscher, C., Allen, D., Crawford, J., 2010. Application of OMI observations to a space-based indicator of NO_x and VOC controls on surface ozone formation. Atmos. Environ. 44, doi:10.1016/j.atmosenv.2010.03.010, 2213-2223.

Duncan, B., Yoshida, Y., de Foy, B., Lamsal, L., Streets, D., Lu, Z., Pickering, K., Krotkov, N., 2013. The observed response of Ozone Monitoring Instrument (OMI) NO_2 columns to NO_x emission controls on power plants in the United States: 2005-2011. Atmos. Environ. 81, doi:10.1016/jatmosenv.2013.08.068, 2013.

de Foy, B., Krotkov, N., Bei, N., Herndon, S., Huey, L., Martínez, A.-P., Ruiz-Suárez, L., Wood, E., Zavala, M., and Molina, L., 2009. Hit from both sides: tracking industrial and volcanic plumes in Mexico City with surface measurements and OMI SO_2 retrievals during the MILAGRO field campaign. Atmos. Chem. Phys. 9, 9599-9617, doi:10.5194/acp-9-9599-2009,.

de Laat, A. T. J., Aben, I., and Roelofs, G. J., 2005. A model perspective on total tropospheric O_3 column variability and implications for satellite observations. J. Geophys. Res. 110, D13303, doi:10.1029/2004JD005264.

Engel-Cox, J., Holloman, C., Coutant, B., Hoff, R., 2004. Qualitative and quantitative evaluation of MODIS satellite sensor data for regional and urban scale air quality. Atmospheric Environment, 38, 16, 2495-2509.

EPA, 2012. Our Nation's Air: Status and Trends through 2010. Environmental Protection Agency. EPA-454/R-12-001.

Federal Register, 2007. Treatment of data influenced by exceptional events. Final rule. Federal Register, 40 CFR Parts 50 and 51, Vol. 72, No. 55, Thursday, March 22, 2007; http://www.epa.gov/ttn/caaa/t1/fr_notices/exeventfr.pdf.

Fioletov, V.E., McLinden, C.A., Krotkov, N., Moran, M.D., Yang, K., 2011. Estimation of SO_2 emissions using OMI retrievals. Geophys. Res. Lett. 38, L21811.

Fioletov, V. E., McLinden, C.A., Krotkov, N., Yang, K., Loyola, D.G., Valks, P., Theys, N., Van Roozendael, M., Nowlan, C.R., Chance, K., Liu, X., Lee, C., and Martin, R.V., 2013. Application of OMI, SCIAMACHY, and GOME-2 satellite SO_2 retrievals for detection of large emission sources, J. Geophys. Res. Atmos. 118, doi:10.1002/jgrd.50826.

Fiore, A., Bradley Pierce, R., Dickerson, R., Lin, M., 2014. Detecting and attributing episodic high background ozone events. Accepted to Environmental Manager.

Fishman, J., Wozniak, A. E., and Creilson, J. K., 2003. Global distribution of tropospheric ozone from satellite measurements using the empirically corrected tropospheric ozone residual technique: Identification of the regional aspects of air pollution. Atmos. Chem. Phys., 3, 893-907, doi:10.5194/acp-3-893-2003.

Fishman, J., Bowman, K.W., Burrow, J.P., Richter, A., Chance, K.V., Edwards, D.P., Martin, R.V., Morris, G.A., Pierce, R.B., Ziemke, J.R., Al-Saadi, J.A., Creilson, J.K., Schaack, T.K.,

Thompson, A.M., 2008. Remote sensing of tropospheric pollution from space, Bulletin of the American Meteorological Society, 805-821. doi:10.1175/2008BAMS2526.1.

Fishman, J., et al., 2012. The United States' Next Generation of Atmospheric Composition and Coastal Ecosystem Measurements: NASA's Geostationary Coastal and Air Pollution Events (GEO-CAPE) Mission. Bull. Amer. Meteor. Soc. 93, 1547-1566, 2012, doi:10.1175/BAMS-D-11-00201.1.

Flynn, C., Pickering, K., Crawford, J., Lamsal, L., Krotkov, N., Herman, J., Weinheimer, A., Chen, G., Liu, X., Szykman, J., Tsay, S.-C., Loughner, C., Hains, J., Lee, P., Dickerson, R., Stehr, J., Brent, L., 2014. The Relationship between Column-density and Surface Mixing Ratio: Statistical Analysis of O_3 and NO_2 Data from the July 2011 Maryland DISCOVER-AQ Mission. Submitted to Atmospheric Environment.

Gupta, P., Christopher, S., 2009. Particulate matter air quality assessment using integrated surface, satellite, and meteorological products: Multiple regression approach, J. Geophys. Res. 114, D14205, doi:10.1029/2008JD011496.

Hair, J., Hostetler, C., Cook, A., Harper, D., Ferrare, R., Mack, T., Welch, W., Izquierdo, L., Hovis, F., 2008. Airborne High Spectral Resolution Lidar for profiling aerosol optical properties. Appl. Optics 47, 6734-6752, 10.1364/AO.47.006734.

He, H., Stehr, J. W., Hains, J. C., Krask, D. J., Doddridge, B. G., Vinnikov, K. Y., Canty, T. P., Hosley, K. M., Salawitch, R. J., Worden, H. M., Dickerson, R. R., 2013. Trends in emissions and concentrations of air pollutants in the lower troposphere in the Baltimore/Washington airshed from 1997 to 2011. Atmospheric Chemistry and Physics 13, 7859-7874. doi:10.5194/acp-13-7859-2013.

Hilsenrath, E., Chance, K., 2013. NASA ups the TEMPO on monitoring air pollution. The NASA Earth Observer, 25, 2, p. 10-13, http://eospso.gsfc.nasa.gov/sites/default/files/eo_pdfs/March_April_2013_508_color.pdf.

Hoff, R., Christopher, S., 2009. Remote Sensing of Particulate Pollution from Space: Have We Reached the Promised Land? J. Air Waste Manage. Assoc. 59(6), 645-675.

Holben, B., et al., 1998. AERONET – a federated instrument network and data archive for aerosol characterization, Remote Sens. Environ., 66, 1-16.

Holben, B., et al., 2001. An emerging ground-based aerosol climatology: aerosol optical depth from AERONET, J. Geophys. Res., 106, 12067-12097.

Hooghiemstra, P.B., Krol, M.C., Bergamaschi, P., de Laat, A.T.J., van der Werf, G.R., Novelli, P.C., Deeter, M.N., Aben, I., Röckmann, T., 2012. Comparing optimized CO emission estimates using MOPITT or NOAA surface network observations. J. Geophys. Res. 117, D06309, doi:10.1029/2011JD017043.

Hostetler, C., et al., Airborne Multi-wavelength High Spectral Resolution Lidar for Process Studies and Assessment of Future Satellite Remote Sensing Concepts, in American Geophysical Union. 2012: San Francisco, CA.

Hu, X, Waller, L., Al-Hamdan, M., Crosson, W., Estes Jr, M., Estes, S., Quattrochi, D., Sarnat, J., Liu, Y., 2013. Estimating ground-level PM2.5 concentrations in the southeastern U.S. using geographically weighted regression. Environ Res. 121:1-10.

Hu, X., Waller, L., Lyapustin, A., Wang Y., Al-Hamdan, M., Crosson, W., Estes, M., Estes, S., Quattrochi, D., Puttaswamy, S., Liu, Y., 2014. Estimating Ground-Level PM2.5 Concentrations in the Southeastern United States Using MAIAC AOD Retrievals and a Two-Stage Model. Remote Sens Environ. 140:220-232.

Hudman, R.C., Moore, N.E., Mebust, A.K., Martin, R.V., Russell, A.R., Valin, L.C., Cohen, R.C., 2012. Steps towards a mechanistic model of global soil nitric oxide emissions: implementation and space-based constraints. Atmospheric Chemistry and Physics 12, 7779–7795.

Ichoku, C., Kahn, R., Chin, M., 2012. Satellite contributions to the quantitative characterization of biomass burning for climate modeling. Atmosph. Res., doi:10.1016/j.atmosres.2012.03.007.

Jiang, X., Liu, Y., Yu, B., Jiang, M., 2007. Comparison of MISR aerosol optical thickness with AERONET measurements in Beijing metropolitan area. Remote Sens. Environ. 107, 45-53.

Kahn, R., Gaitley, B., Garay, M., Diner, D., Eck, T., Smirnov, A., Holben, B., 2010. Multiangle Imaging SpectroRadiometer global aerosol product assessment by comparison with the Aerosol Robotic Network. J. Geophys. Res. 115, D23209, doi:10.1029/2010JD014601.

Kahn, R., 2012. Reducing the uncertainties in direct aerosol radiative forcing. Surveys in Geophysics 33:701–721, doi:10.1007/s10712-011-9153-z.

Kar, J., Fishman, J., Creilson, J.K., Richter, A., Ziemke, J., Chandra, S., 2010. Are there urban signatures in the tropospheric ozone column products derived from satellite measurements? Atmos. Chem. Phys. 10, 5213-5222, doi:10.5194/acp-10-5213-2010.

Kasibhatla, P., Chameides, W., Duncan, B., Houyoux, M., Jang, C., Mathur, R., Odman, T., Xiu, A., 1997. Impact of Inert Organic Nitrate Formation on Ground-level Ozone in a Regional Air Quality Model Using the Carbon Bond Mechanism 4, Geophys. Res. Lett. 24, 24.

Kaynak, B., Hu, Y., Martin, R.V., Sioris, C.E., Russell, A.G., 2009. Comparison of weekly cycle of NO_2 satellite retrievals and NO_x emission inventories for the continental United States. J. Geophys. Res. 114, D05302, doi:10.1029/2008JD010714.

Kim, S.-W., Heckel, A., McKeen, S.A., Frost, G.J., Hsie, E.-Y., Trainer, M.K., Richter, A., Burrows, J.P., Peckham, S.E., Grell, G.A., 2006. Satellite-observed U.S. power plant NO_x emission reductions and their impact on air quality. Geophys. Res. Lett. 33, L22812, doi:10.1029/2006GL027749.

Kim, S.-W., Heckel, A., Frost, G.J., Richter, A., Gleason, J., Burrows, J.P., McKeen, S., Hsie, E.-Y., Granier, C., Trainer, M., 2009. NO_2 columns in the western United States observed from space and simulated by a regional chemistry model and their implications for NO_x emissions. J. Geophys. Res. 114, D11301, doi:10.1029/2008JD011343.

Kloog, I., P. Koutrakis, B. A. Coull, H. J. Lee, and J. Schwartz, 2011. Assessing temporally and spatially resolved PM(2.5) exposures for epidemiological studies using satellite aerosol optical depth measurements, Atmospheric Environment, 45(35), 6267-6275.

Knapp, K., Frouin, R., Kondragunta, S., Prados, A., 2005. Toward aerosol optical depth retrievals over land from GOES visible radiances: determining surface reflectance. International Journal of Remote Sensing, 26, 4097-4116.

Knepp, T., Pippin, M., Crawford, J., Chen, G., Szykman, J., Long, R., Cowen, L., Cede, A., Abuhassan, N., Herman, J., Delgado, R., Compton, J., Berkoff, T., Fishman, J., Martins, D., Stauffer, R., Thompson, A. M., Weinheimer, A., Knapp, D., Montzka, D., Lenschow, D., Neil, D., 2013. Estimating surface NO_2 and SO_2 mixing ratios from fast-response total column observations and potential application to geostationary missions. J Atmos. Chem., doi:10.1007/s10874-013-9257-6.

Korontzi, S., McCarty, J., Justice, C., 2008. Monitoring agricultural burning in the Mississippi River Valley region from the Moderate Resolution Imaging Spectroradiometer (MODIS). J. of the Air & Waste management Association, 58, 9, p. 1235-9, doi: 10.3155/1047-3289.58.9.1235.

Lamsal, L.N., Martin, R.V., van Donkelaar, A., Steinbacher, M., Celarier, E.A., Bucsela, E., Dunlea, E.J., Pinto, J., 2008. Ground-level nitrogen dioxide concentrations inferred from the satellite-borne Ozone Monitoring Instrument. J. Geophys. Res., 113, D16308, doi:10.1029/2007JD009235.

Lamsal, L., Martin, R., van Donkelaar, A., Celarier, E., Boersma, R., Dirksen, R., Luo, C., Wang, Y., 2010. Indirect validation of tropospheric nitrogen dioxide retrieved from the OMI satellite instrument: Insight into the seasonal variation of nitrogen oxides at northern midlatitudes. J. Geophys. Res. 115, D05302, doi:10.1029/2009JD013351.

Lamsal, L. N., Martin, R. V., van Donkelaar, A., Celarier, E. A., Bucsela, E. J., Boersma, K. F., Dirksen, R., Luo, C., Wang, Y., 2010. Indirect validation of tropospheric nitrogen dioxide retrieved from the OMI satellite instrument: Insight into the seasonal variation of nitrogen oxides at northern midlatitudes. J. Geophys. Res., 115, D05302. doi:10.1029/2009JD013351.

Lamsal, L.N., Martin, R.V., Padmanabhan, A., van Donkelaar, A., Zhang, Q., Sioris, C.E., Chance, K., Kurosu, T.P., Newchurch, M.J., 2011. Application of satellite observations for timely updates to global anthropogenic NO_x emission inventories. Geophysical Research Letters, 28, L05810.

Langford, A., Aikin, K., Eubank, C., Williams, E., 2009. Stratospheric contribution to high surface ozone in Colorado during springtime, Geophysical Research Letters 36, L12801. doi:10.1029/2009GL038367.

Langford, A. O., et al, 2012. Stratospheric influence on surface ozone in the Los Angeles area during late spring and early summer of 2010, J. Geophys. Res. 117, D00V06. doi:10.1029/2011JD016766.

Lee, H., Liu, Y., Coull, B. Schwartz, J.,Koutrakis, P., 2011. A novel calibration approach of MODIS AOD data to predict PM(2.5) concentrations, Atmospheric Chemistry and Physics, 11(15), 7991-8002.

Lefohn, A.S., et al., 2011. The importance of stratospheric-tropospheric transport in affecting surface ozone concentrations in the western and northern tier of the United States, Atmospheric Environment. doi:10.1016/j.atmosenv.2011.06.014.

Leue, C., Wenig, M., Wagner, T., Klimm, O., Platt, U., Jahne, B., 2001. Quantitative analysis of NO_x emissions from GOME satellite image sequences, J. Geophys. Res. 106, 5493–5505.

Levelt, P.F., van den Oord, G.H.J., Dobber, M.R., Mälkki, A., Visser, H., de Vries, J., Stammes, P., Lundell, J.O.V., Saari, H., 2006. The Ozone Monitoring Instrument. IEEE Transactions on Geoscience and Remote Sensing, 44, 5, 1092-1101.

Li, C., Joiner, J., Krotkov, N., Bhartia, P. K., 2013. A fast and sensitive new satellite SO_2 retrieval algorithm based on principal component analysis: Application to the Ozone Monitoring Instrument. Geophysical Research Letters 40, doi:10.1002/2013GL058134.

Lin M., A. Fiore, A., Cooper, O., Horowitz , L., A. Langford, A., Levy II , H., Johnson, B., Naik, V., Oltmans, S., Senff, C., 2012. Springtime high surface ozone events over the western United States: Quantifying the role of stratospheric intrusions, J. Geophys. Res. 117, D00V22, doi:10.1029/2012JD018151.

Liu, Y., Park, R., Jacob, D. Li, Q., Kilaru, V., Sarnat, J., 2004. Mapping annual mean ground-level PM2.5 concentrations using Multiangle Imaging Spectroradiometer aerosol optical thickness over the contiguous United States, J. Geophys. Res. 109(D22), Art. No. D22206.

Liu, Y., Sarnat, J., Kilaru, V., Jacob, D., Koutrakis, P., 2005. Estimating Ground-Level PM2.5 in the Eastern United States Using Satellite Remote Sensing, Environ. Sci. Technol. 39(9), 3269 - 3278.

Liu, Y., R. Kahn, and P. Koutrakis, 2007a. Estimating PM2.5 Component Concentrations and Size Distributions Using Satellite Retrieved Fractional Aerosol Optical Depth: Part I - Method Development, J. Air & Waste Manage. Assoc., 57(11), 1351-1359.

Liu, Y., R. Kahn, S. Turquety, R. M. Yantosca, and P. Koutrakis, 2007b. Estimating PM2.5 Component Concentrations and Size Distributions Using Satellite Retrieved Fractional Aerosol Optical Depth: Part II - A Case Study, J. Air & Waste Manage. Assoc., 57(11), 1360-1369.

Liu, Y., Paciorek, C., Koutrakis, P., 2009. Estimating Regional Spatial and Temporal Variability of PM2.5 Concentrations Using Satellite Data, Meteorology, and Land Use Information, Environ. Health Perspect., 117(6), 886-892.

Lu, Z., Streets, D., 2012. Increase in NO_x emissions from Indian thermal power plants during 1996-2010: Unit-based inventories multisatellite observations. Environmental Science & Technology 46, 7463-7470, dx.doi.org/10.1021/es300831w.

Lyapustin, A., Martonchik, J., Wang, Y., Laszlo, I., Korkin, S., 2011a. Multi-Angle Implementation of Atmospheric Correction (MAIAC): Part 1. Radiative Transfer Basis and Look-Up Tables, J. Geophys. Res., 116, 2011a. D03210,doi:10.1029/2010JD014985.

Lyapustin, A., Wang, Y., Laszlo, I., Kahn, R., Korkin, S., Remer., L., Levy, R., Reid, J., 2011b. Multi-Angle Implementation of Atmospheric Correction (MAIAC): Part 2. Aerosol Algorithm, J. Geophys. Res., 116, D03211, 2011b, doi:10.1029/2010JD014986.

Martin, R. V., Parrish, D. D., Ryerson, T. B., Nicks Jr., D. K., Chance, K., Kurosu, T. P., Jacob, D. J., Sturges, E. D., Fried, A., Wert, B. P., 2004. Evaluation of GOME satellite measurements of tropospheric NO_2 and formaldehyde using regional data from aircraft campaigns in the southeastern United States, Journal Geophysical Research 109, D24307. doi:10.1029/2004JD004869.

Martin, R., Sauvage, B., Folkins, I., Sioris, C., Boone, C., Bernath, P., Ziemke, J., 2007. Space-based constraints on the production of nitric oxide by lightning. J. Geophys. Res., 112, D09309, doi:10.1029/2006JD007831.

Martin, R., 2008. Satellite remote sensing of surface air quality. Atmospheric Environment, 42, 7823-43, doi:10.1016/j.atmosenv.2008.07.018.

McLinden, C.A., Fioletov, V., Boersma, K.F., Krotkov, N., Sioris, C.E., Veefkind, J.P., Yang, K., 2012. Air quality over the Canadian oil sands: A first assessment using satellite observations. Geophys. Res. Lett.39, L04804.

Millet, D. B., D. J. Jacob, K. F. Boersma, T.-M. Fu, T. P. Kurosu, K. Chance, C. L. Heald, and A. Guenther, 2008. Spatial distribution of isoprene emissions from North America derived from formaldehyde column measurements by the OMI satellite sensor, J. Geophys. Res. 113, D02307. doi:10.1029/2007JD008950.

Molod, A., Takacs, L., Suarez, M., Bacmeister, J., Song, I.-S., Eichmann, A., 2012. The GEOS-5 Atmospheric General Circulation Model: Mean Climate and Development from MERRA to Fortuna. NASA/TM–2012-104606, Technical Report Series on Global Modeling and Data Assimilation, Vol. 28, *M. Suarez, Editor:* http://gmao.gsfc.nasa.gov/pubs/docs/tm28.pdf.

Munchak, L., Levy, R., Mattoo, S., Remer, L., Holben, B., Schafer, J., Hostetler, C., Ferrare, R.A., 2013. MODIS 3 km aerosol product: applications over land in an urban/suburban region. Atmos. Meas. Tech. 6, 1747-1759.

NASA Applied Sciences Annual Report, 2012. http://appliedsciences.nasa.gov/pdf/2012AnnualReport_508.pdf.

NSTC, November 2013, Air Quality Observation Systems in the United States, Product of the Committee on Environment, Natural Resources, and Sustainability, National Science and Technology Council (NSTC), http://www.whitehouse.gov/sites/default/files/microsites/ostp/NSTC/air_quality_obs_2013.pdf .

Ott, L., Duncan, B., Pawson, S., Colarco, P., Chin, M., Randles, C., Diehl, T., Nielsen, J., 2010. Influence of the 2006 Indonesian biomass burning aerosols on tropical dynamics studied with the GEOS-5 AAGCM. J. Geophys. Res. 115, D14121, doi:10.1029/2009JD013181.

Palmer, P. I., Jacob, D. J., Chance, K., Martin, R. V., Spurr, R. J. D., Kurosu, T. P., Bey, I., Yantosca, R., Fiore, A., Li, Q., 2001. Air mass factor formulation for spectroscopic measurements from satellites: Application to formaldehyde retrievals from the Global Ozone Monitoring Experiment. J. Geophys. Res., 106(D13), 14539–14550, doi:10.1029/2000JD900772.

Palmer, P. I., Jacob, D. J., Fiore, A. M., Martin, R. V., Chance, K., Kurosu, T. P., 2003. Mapping isoprene emissions over North America using formaldehyde column observations from space, J. Geophys. Res. 108(D6), 4180. doi:10.1029/2002JD002153.

Palmer, P.I., Abbot, D.S., Fu, T.-M., Jacob, D.J., Chance, K., Kurosu, T.P., Guenther, A., Wiedinmyer, C., Stanton, J.C., Pilling, M.J., Pressley, S.N., Lamb, B., Sumner, A.L., 2006. Quantifying the seasonal and interannual variability of North American isoprene emissions using satellite observations of the formaldehyde column. J. Geophys. Res. 111, D12315. doi:10.1029/2005JD006689.

Patadia, F., Kahn, R., Limbacher, J., Burton, S., Ferrare, R., Hostetler, C., Hair, J., 2013. Aerosol Airmass Type Mapping Over the Urban Mexico City Region From Space-based Multi-angle Imaging. Atm. Chem. Phys. 13, 9525–9541.

Pawson, S., R. Stolarski, A. Douglass, P. Newman, J. Nielsen, S. Frith, M. Gupta, 2008. Goddard Earth Observing System chemistry-climate model simulations of stratospheric ozone-temperature coupling between 1950 and 2005. J. Geophys. Res. 113, D12103, doi: 10.1029/2007JD009511.

Pelletier, B., Santer, R., Vidot, J., 2007. Retrieving of particulate matter from optical measurements: A semiparametric approach. J. Geophys. Res. 112, D06208, doi:10.1029/2005JD006737.

Prados, A. I., Kondragunta, S., Ciren, P., Knapp, K., 2007. The GOES Aerosol/ Smoke Product (GASP) over North America: Comparisons to AERONET and MODIS Observations. J. Geophys. Res. 112, D15201 doi:10.1029/2006JD007968.

Prados, A. I., et al., May 2010. Access, Visualization, and Interoperability of Air Quality Remote Sensing Data Sets Via the Giovanni Online Tool, Special Issue on Heterogeneous data access and use for geospatial user communities, IEEE Journal of Selected Topics in Earth Observations and Remote Sensing, JSTARS).

Prados, A. I., October 3, 2012. NASA’s ARSET Training Program: From the Classroom to Real-World Satellite Applications, Earthzine Magazine October Highlight.

Rienecker, M., Suarez, M., Gelaro, R., et al., 2011. MERRA - NASA's Modern-Era Retrospective Analysis for Research and Applications. J. Climate 24, 3624-3648, doi: 10.1175/JCLI-D-11-00015.1.

Russell, A.R., Valin, L.C., Cohen, R.C., 2012. Trends in OMI NO_2 observations over the United States: effects of emission control technology and the economic recession. Atmospheric Chemistry and Physics 12, 12197–12209.

Schaap, M., Apituley, A., Timmermans, R., Koelemeijer, R., de Leeuw, G., 2009. Exploring the relation between aerosol optical depth and PM2.5 at Cabauw, the Netherlands, Atmospheric Chemistry and Physics, 909-925.

Scheffe, R.D., Solomon, P.A., Husar, R., Hanley, T., Schmidt, M., Koerber, M., Gilroy, M., Hemby, J., Watkins, N., Papp, M., Rice, J., Tikvart, J., and Valentinetti, R., 2012. The National Ambient Air Monitoring Strategy: Rethinking the Role of National Networks, Journal of the Air & Waste Management Association, 59:5, 579-590, DOI: 10.3155/1047-3289.59.5.579

Sillman, S., 1995. The use of NO_y, H_2O_2, and HNO_3 as indicators for ozone-NO_x-hydrocarbon sensitivity in urban locations, J. Geophys. Res., 100, 14175-14188.

Streets, D., Canty, T., Carmichael, G., de Foy, B., Dickerson, R., Duncan, B., Edwards, D., Haynes, J., Henze, D., Houyoux, M., Jacob, D., Krotkov, N., Lamsal, L., Liu, Y., Lu, Z., Martin, R., Pfister, G., Pinder, R., Salawitch, R., Wecht, K., 2013. Emissions estimation from satellite retrievals: A review of current capability, Atmos. Environ., doi: 10.1016/j.atmosenv.2013.05.051.

van Donkelaar, A., R. V. Martin, M. Brauer, R. Kahn, R. Levy, C. Verduzco, and P. J. Villeneuve, 2010. Global Estimates of Ambient Fine Particulate Matter Concentrations from Satellite-Based Aerosol Optical Depth: Development and Application, Environ. Health Perspect., 118(10), 847-855.

Velders, G. J. M., Granier, C., Portmann, R. W., Pfeilsticker, K., Wenig, M., Wagner, T., Platt, U., Richter, A., Burrows, J. P., 2001. Global tropospheric NO_2 column distributions: Comparing 3-D model calculations with GOME measurements, J. Geophys. Res., 106, 12,643–12,660.

Wang, J., Christopher, S., 2003. Intercomparison between satellite-derived aerosol optical thickness and $PM_{2.5}$ mass: Implications for air quality studies. Geophysical Research Letters, 30, 2095, doi:10.1029/2003GL018174, 21.

Witte, J., Schoeberl, M., Douglass, A., Gleason, J., Krotkov, N., Gille, J., Pickering, K., Livesey, N., 2009. Satellite observations of changes in air quality during the 2008 Beijing Olympics and Paralympics. Geophys. Res. Lett. 36, L17803.

Worden, J., Liu, X., Bowman, K., Chance, K., Beer, R., Eldering, A., Gunson, M., Worden, H., 2007. Improved tropospheric ozone profile retrievals using OMI and TES radiances. Geophys. Res. Lett. 34, L01809, doi:10.1029/2006GL027806.

Worden, H.M., et al., 2013. Decadal record of satellite carbon monoxide observations. Atmospheric Chemistry and Physics 13, 837-850. doi:10.5194/acp-13-837-2013.

Yates, E. L., Iraci, L. T., Roby, M. C., Pierce, R. B., Johnson, M. S., Reddy, P. J., Tadić, J. M., Loewenstein, M., Gore, W., 2013. Airborne observations and modeling of springtime stratosphere-to-troposphere transport over California, Atmos. Chem. Phys. Discuss. 13, 10157-10192, doi:10.5194/acpd-13-10157-2013.

Zhang, H., Hoff, R., Engel-Cox, J., 2009. The relation between Moderate Resolution Imaging Spectroradiometer (MODIS) aerosol optical depth and $PM_{2.5}$ over the United States: a geographical comparison by EPA regions, Journal of Air & Waste management Association 59, 1358-1369.

Ziemba L., et al., 2013. Airborne observations of aerosol extinction by in situ and remote-sensing techniques: Evaluation of particle hygroscopicity. Geophys. Res. Lett. 40, 417–422, doi:10.1029/2012GL054428.

Zoogman, P., Jacob, D., Chance, K., Zhang, L., Le Sager, P., Fiore, A., Eldering, A., Liu, X., Natraj, V., Kulawik, S., 2011. Ozone Air Quality Measurement Requirements for a Geostationary Satellite Mission. Atmos. Environ. 45, 7,143-7,150.

Appendices

Appendix A. Satellite prediction of surface $PM_{2.5}$ levels

Despite the complexity of the AOD-$PM_{2.5}$ relationship (e.g., Case Example #1 in Section 2.1), AOD data from satellite instruments have been shown to correlate well with $PM_{2.5}$ data from surface monitors in some regions of the U.S., such as the eastern U.S.; Hoff and Christopher (2009) provide a comprehensive summary of these relations that were reported in the literature. For practical use of AOD as a proxy for $PM_{2.5}$, several linear and nonlinear regression models between AOD and $PM_{2.5}$ have been developed for specific regions or cities (e.g., Pelletier et al., 2007; Schaap et al., 2009; Zhang et al., 2009). Various statistical models ranging from simple univariate regression to complex hierarchical models introduce effect-modifiers, such as season, temperature, relative humidity and land use parameters to account for the impact of changing aerosol composition and horizontal / vertical mixing (Gupta and Christopher, 2009; Kloog et al., 2011; Lee et al., 2011; Liu et al., 2005, 2009). The latest statistical models are able to predict daily $PM_{2.5}$ concentrations with a 20-30% relative error, but require the support of an extensive ground monitoring network (Hu et al., 2013, 2014). Another approach uses aerosol vertical profiles simulated by models to account for the changing AOD-$PM_{2.5}$ over time and space, therefore eliminating the need for ground observations and allowing model applications in regions with extremely sparse or no routine AQ monitoring (Liu et al., 2004; van Donkelaar et al., 2010). However, this method currently has higher prediction errors and the spatial resolution of predicted $PM_{2.5}$ data is limited by both the satellite data and models.

Satellite prediction of surface $PM_{2.5}$ levels is still under development. There is no gold standard or universally applicable modeling approach. A few rules of thumb are provided here. First, because the AOD-$PM_{2.5}$ relationship varies in space and time, it is generally true that more complex multivariate models will have more robust performance (i.e., lower and less variable prediction errors) than simpler linear regression models. The end-user will have a much better chance of getting more accurate annual mean estimates than daily levels. Second, the satellite $PM_{2.5}$ models that use MODIS AOD as the primary predictor cannot be applied in regions with bright surfaces (e.g., western U.S.). Models using specialty sensors, such as the MISR, may

have better performance (Liu et al., 2007a; 2007b), but users must be cautious when estimating very low $PM_{2.5}$ levels. Third, a sophisticated statistical model developed in one region can maintain its structure when transferred to another region, but it may be necessary to re-calibrate it using local data. Finally, different satellite AOD products vary in their value range, accuracy, and spatial resolution. If a user wishes to extend model coverage, validation and calibration must be done before mixing several satellite AOD products.

Appendix B. An "apples-to-apples" comparison of model output to satellite VCD data

For illustrative purposes, an end-user may wish to evaluate a model's distribution of surface NO_2 using the either the L2 or L3 OMI tropospheric NO_2 product. One may sum all NO_2 molecules of a pollutant in a vertical column in their model to calculate the model's VCD (VCD_M), which could be directly compared to the VCD in the satellite data file (VCD_D). This straight-forward approach may be adequate for many applications, particularly for qualitative comparisons. However, doing so assumes minimal influence from the "initial guess" (i.e., an assumed vertical profile of the concentration of the gas in the atmosphere) that is used in the retrieval algorithm. The initial guess is usually taken from a model global climatology. The influence of this initial guess remains in varying degrees in the final product. Therefore, it is generally better to perform one additional step to ensure an "apples-to-apples" comparison of VCD_M and VCD_D by removing the influence of the initial guess. This additional step is straight-forward to perform and is critical for making quantitative inferences.

To remove the influence of the initial guess, one must first use the variable called "scattering weight" that is included in the OMI NO_2 data files along with VCD_D. (For some products, such as those from IR instruments, the data files may not include "scattering weight", but instead a related variable called "averaging kernel".) Scattering weights are provided for various pressure levels from the surface to the top of the atmosphere. They uniquely depend on satellite viewing geometry, surface albedo, the presence of aerosols and clouds, etc. The end-user must sum over all model layers the product of the scattering weight and model partial column (molecules/cm^2) in each model layer. This sum divided by VCD_M is called the air mass factor (AMF) of the model (AMF_M). Second, the end-user must divide the product of VCD_D and AMF_D from the data file by AMF_M to obtain a modified form of VCD_D (VCD'_D): $VCD'_D = (VCD_D * AMF_D)/AMF_M$. By performing these two steps, one obtains a consistent estimate (i.e.,

no influence of the initial guess) of VCD'_D using the ratio of AMF_D and AMF_M. Therefore, one may now fairly compare VCD'_D with VCD_M. For more information on this complicated relationship, the reader is referred to Palmer et al. (2001). It is always a good idea to contact the data developers for guidance in using their products and properly comparing the data to a model's output.

Tables

Table 1. Frequently used acronyms and terms.

Acronym/Name	Phrase/Description
AQAST	NASA *Air Quality Applied Sciences Team*; http://acmg.seas.harvard.edu/aqast/
ARSET	NASA *Applied Remote SEnsing Training*; http://airquality.gsfc.nasa.gov/
Chemical Species	
AOD	*Aerosol Optical Depth*, also referred to as Aerosol Optical Thickness (AOT)
NO_x	*Nitrogen oxides*, the sum of NO and NO_2
PM, $PM_{2.5}$	*Particulate Matter*, < 2.5 μm in aerodynamic diameter
SO_2	*Sulfur dioxide*
VOCs	*Volatile Organic Compounds*
Agencies	
EPA	*Environmental Protection Agency*
ESA	*European Space Agency*
EUMETSAT	*European Organisation for the Exploitation of Meteorological Satellites*
NASA	*National Aeronautics and Space Administration*
NOAA	*National Oceanic and Atmospheric Administration*
Instruments/Missions[a]	
AIRS	NASA Aqua *Atmospheric Infrared Sounder*
DISCOVER-AQ	NASA *Deriving Information on Surface conditions from Column and Vertically Resolved Observations Relevant to Air Quality* field mission; http://www.nasa.gov/mission_pages/discover-aq/
GASP	*GOES East Aerosol/Smoke Product* on the NOAA GOES East satellite; http://www.ssd.noaa.gov/PS/FIRE/GASP/gasp.html
GOES	NOAA *Geostationary Operational Environmental Satellite*
GOME	*Global Ozone Monitoring Experiment* on the ESA ERS-2 satellite; https://earth.esa.int/web/guest/missions/esa-operational-eo-missions/ers/instruments/gome
GOME-2	*Global Ozone Monitoring Experiment-2* on the EUMETSAT Metop-A satellite; http://oiswww.eumetsat.org/WEBOPS/eps-pg/GOME-2/GOME2-PG-0TOC.htm
MISR	NASA Terra *Multi-angle Imaging SpectroRadiometer*
MOPITT	NASA Terra *Measurements of Pollution in the Troposphere*
MODIS	*Moderate Resolution Imaging Spectroradiometer* on the NASA Terra and Aqua satellites
OMI	NASA Aura *Ozone Monitoring Instrument*
SCIAMACHY	*SCanning Imaging Absorption spectroMeter for Atmospheric CHartographY* on the Envisat satellite; http://www.sciamachy.org/
Other	
AQ	*Air Quality*
AQS	EPA *Air Quality System* of monitoring stations
column density	the number of molecules of an atmospheric gas between the satellite instrument and the Earth's surface per area of the Earth's surface
NAAQS	EPA *National Ambient Air Quality Standards*
SCD	*Slant Column Density*
VCD	*Vertical Column Density*

[a] If a website is not provided, the data from a particular instrument may be found via one or more of the websites listed in Table 2.

Table 2. Data discovery, visualization, and analysis resources for the end-user.

Name	Description	Website
ARSET	NASA *Applied Remote SEnsing Training.*	http://airquality.gsfc.nasa.gov/
AQAST	NASA *Air Quality Applied Sciences Team.*	http://acmg.seas.harvard.edu/aqast/
Multi-Purpose*		
EOSDIS	*Earth Observing System Data and Information System.* Useful web tools are available to search data files by instrument and pollutant type.	http://earthdata.nasa.gov
EOSDIS/ LANCE	*Land Atmosphere Near-real-time Capability for EOS* is NASA's main tool for visualization and download of near-real-time data and imagery.	https://earthdata.nasa.gov/data/near-real-time-data/
EOSDIS/ Reverb	Search, access and download data files, with spatial and temporal sub-setting.	http://reverb.echo.nasa.gov/reverb
GES DISC	*Goddard Earth Sciences Data and Information Services Center.* A NASA data center where pollution and aerosol files may be found.	http://disc.sci.gsfc.nasa.gov
GES DISC/ Giovanni	An interactive visualization and analysis web tool.	http://disc.sci.gsfc.nasa.gov/giovanni/
GES DISC/ Mirador	Search on time, space, and keywords for datasets and data files.	http://mirador.gsfc.nasa.gov
LaRC ASDC	*Langley Research Center Atmospheric Science Data Center.* A NASA data center where pollution and aerosol files may be found.	http://eosweb.larc.nasa.gov
LAADS Web	*Level 1 and Atmosphere Archive and Distribution System.* Access MODIS L1, Atmosphere and Land products, and VIIRS L1 and Land products.	http://ladsweb.nascom.nasa.gov
True color imagery and Smoke		
Worldview	An interactive visualization and analysis web tool.	https://earthdata.nasa.gov/labs/worldview/
HMS	NOAA *Hazard Mapping System* Fire and Smoke Product. Access near-real-time data.	http://www.ospo.noaa.gov/Products/land/hms.html
EOSDIS/ FIRMS	*Fire Information for Resource Management System.* Access near-real-time data.	http://earthdata.nasa.gov/data/near-real-time-data/firms
Application Specific		
IDEA	NOAA *Infusing Satellite Data into Environmental Applications*. Near-real-time access to MODIS and GOES aerosol products and meteorological information.	http://www.star.nesdis.noaa.gov/smcd/spb/aq/
IMAPP	NOAA IDEA-I *International MODIS/AIRS Processing Package*. A software package that uses either Terra or Aqua MODIS AOD to identify areas of high aerosol loading from which 48-hr forward trajectories are initialized.	http://cimss.ssec.wisc.edu/imapp/ideai_v1.0.shtml
RSIG	EPA *Remote Sensing Information Gateway*. Facilitates comparisons between NASA imagery and CMAQ model output.	http://ofmpub.epa.gov/rsig/rsigserver?index.html
EE DSS	*Exceptional Event Decision Support System.* Facilitates the analysis of both surface and satellite data for exceptional event demonstrations.	http://www.datafed.net

*There are web tools that provide access to multiple parameters relevant to AQ (e.g., aerosols and gases), data files, and visualizations, and in some cases other features, such as temporal and spatial sub-setting of the data, and limited data analysis

Figures

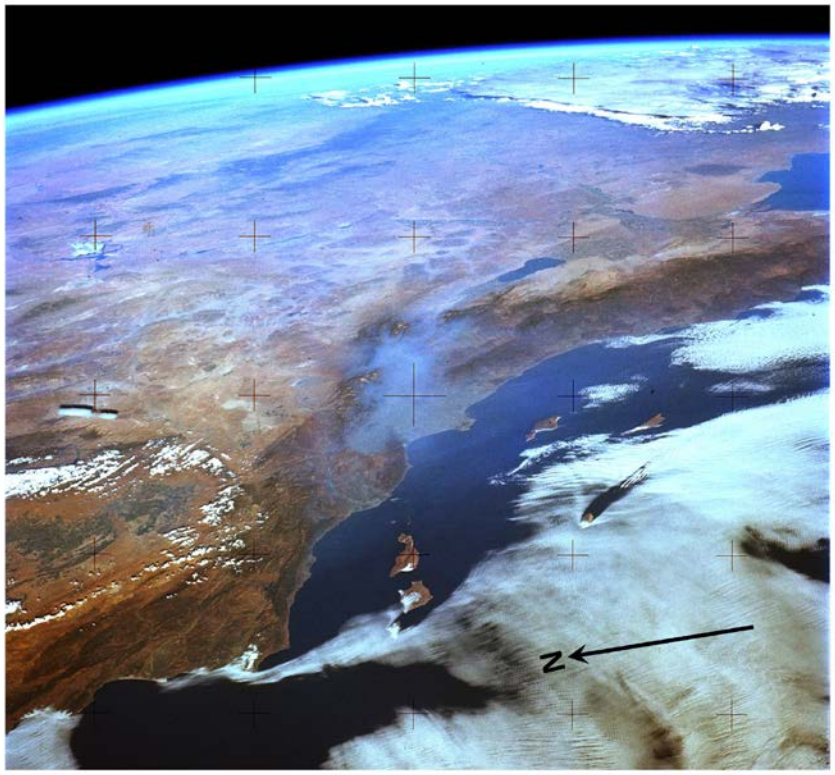

Figure 1. An early photo taken in 1973 from the NASA Skylab space station. It shows a thick layer of smog in the Los Angeles Basin (center of photo). The photo illustrates the "bird's eye" view from space provided by satellites. Photo credit: Image Science & Analysis Laboratory, NASA Johnson Space Center.

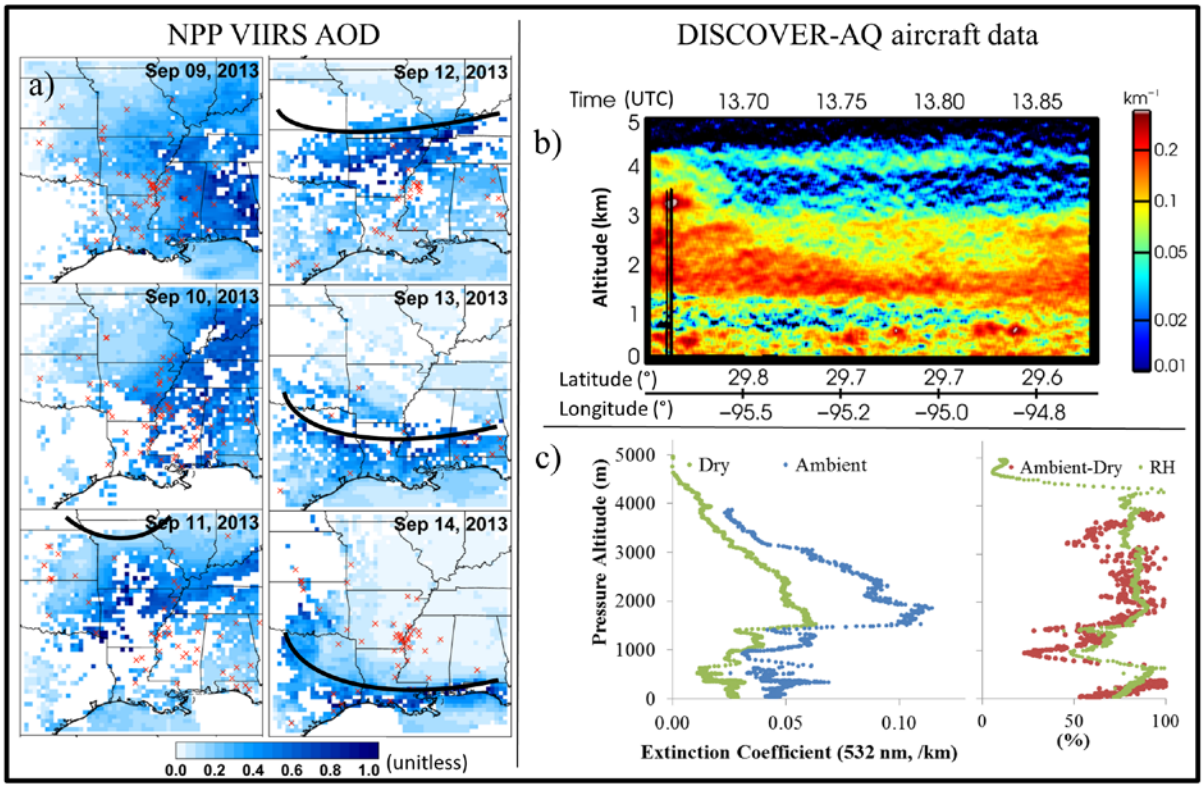

Figure 2. a) The aerosol optical depth (AOD) product (unitless) from the Suomi NPP VIIRS instrument indicates that aerosols, which were partly associated with agricultural fires in the Mississippi Valley, accumulated in the central US and were transported ahead of a cold front to the Gulf Coast, reaching the Houston area on September 14th. The location of each fire detected by VIIRS is shown with a red "x". The black lines show the approximate locations of the cold front at 1:00 pm local time each day. White areas indicate missing data, mainly due to the presence of clouds. b) Aerosol extinction coefficient (532 nm; km^{-1}) data collected on September 14th by the HSRL-2 instrument on an aircraft as part of the NASA DISCOVER-AQ field campaign; the data presented are from a portion of a flight from the "West Houston" surface monitoring site located in Houston to the "Smith Point" surface monitoring site, located about 70 km to the southeast. The transit occurred between 8:30 – 9 am local time or 1:30 – 2 pm UTC. The data confirm that aerosol levels were high regionally, extending to a depth of 3-4 km above the surface, though surface levels of $PM_{2.5}$ as measured by the TCEQ observational network were relatively low, similar to values from previous days. This indicates that the pollution imported into the Houston area from the Mississippi Valley region was located aloft, above a layer of aerosols which is typically found in Houston that is associated with local sources. c) (left) Over the "West Houston" surface monitoring site, the aircraft data of dry extinction coefficient (532 nm, km^{-1}) data collected on September 14th around 8:30 am local time indicate that aerosols levels above 1.5 km (i.e., the imported pollution) were greater than those closer to the surface (i.e., from local sources in the Houston area). However, the data indicate that the ambient scattering was significantly enhanced above 2 km by high relative humidity, inflating the AOD levels. (right) The difference between the ambient and dry aerosol extinction coefficients (%) correlates well with relative humidity (RH; %).

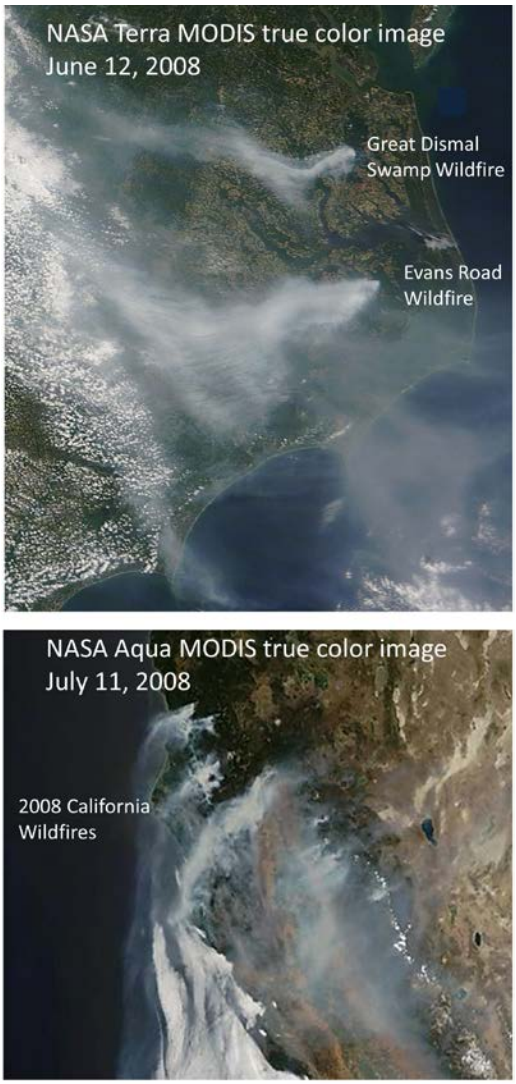

Figure 3. (top) NASA Terra MODIS true color image taken on June 12, 2008, showing widespread smoke pollution from the Great Dismal Swamp and Evans Road wildfires in Virginia and North Carolina. (bottom) NASA Aqua MODIS true color image taken on July 11, 2008, showing extensive smoke from wildfires over northern California.

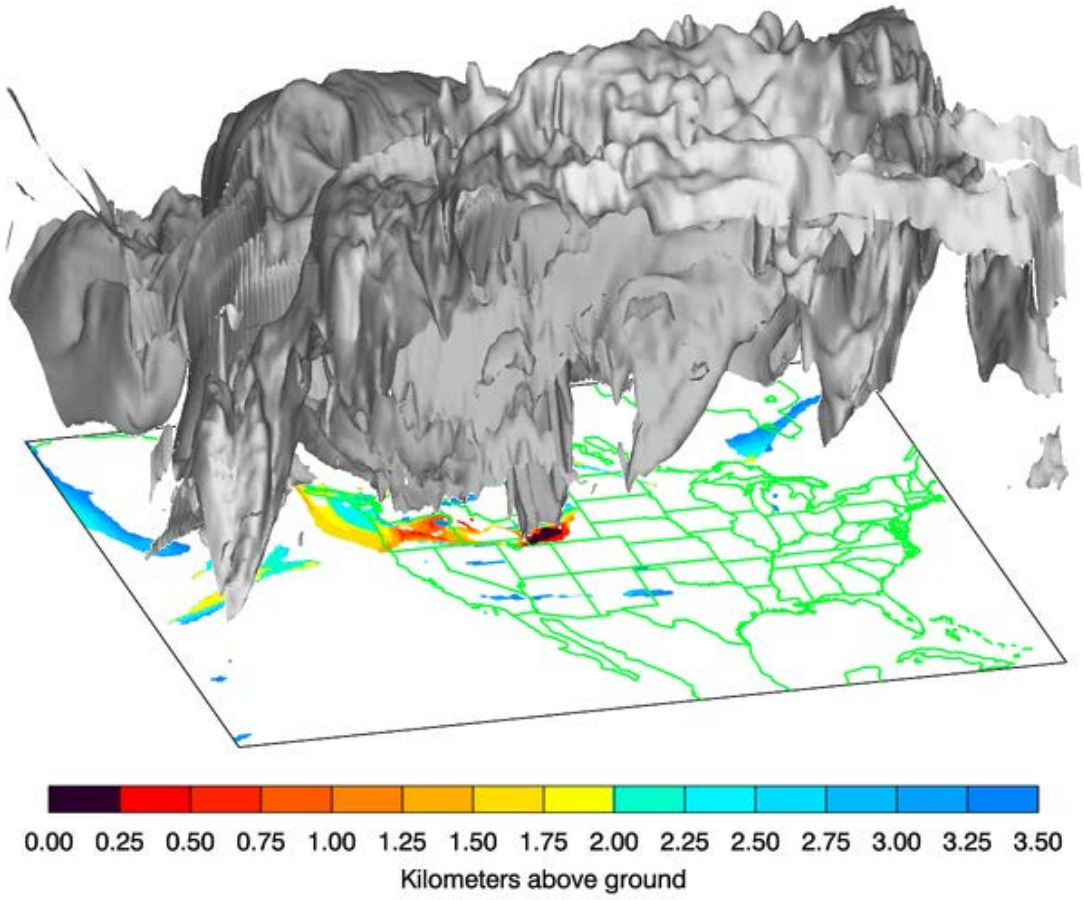

Figure 4. The NASA GEOS-5 chemistry and climate model output shows the location of a stratospheric intrusion that impacted surface AQ in several states in the western U.S., including an AQS site at South Pass, WY, from February 27-28th, 2009. The gray iso-surface depicts the 70 ppbv ozone concentration in the model; higher ozone concentrations are found above this surface. The colors indicate the altitude of the iso-surface above the ground (km).

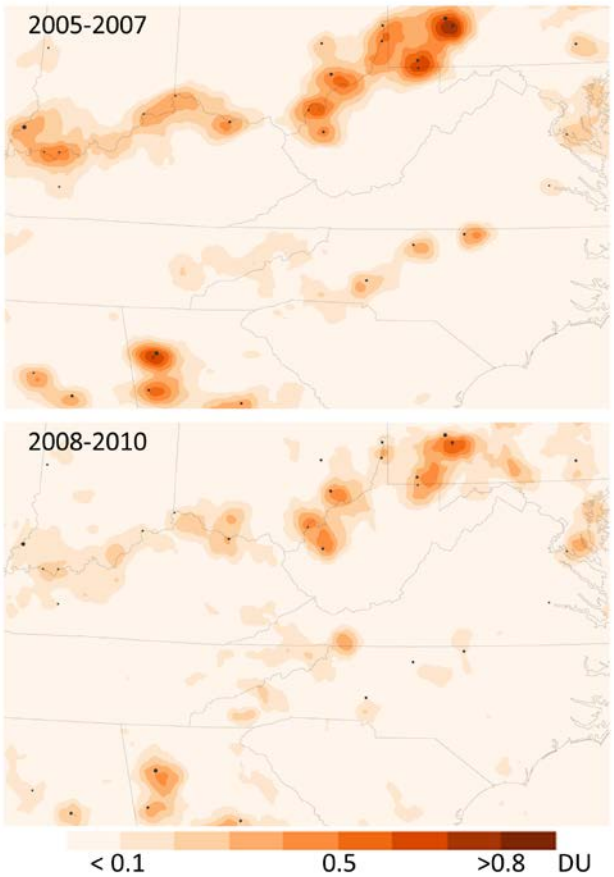

Figure 5. The OMI SO_2 product (DU; 1 DU = 2.69×10^{16} molecules/cm^2) illustrates the success of emission control efforts between 2005 and 2010 at power plants, indicated by dots, in the eastern U.S. (adapted from Fioletov et al., 2011). The averages in both the top and bottom panels are averages of three years each, 2005-2007 and 2008-2010, respectively.

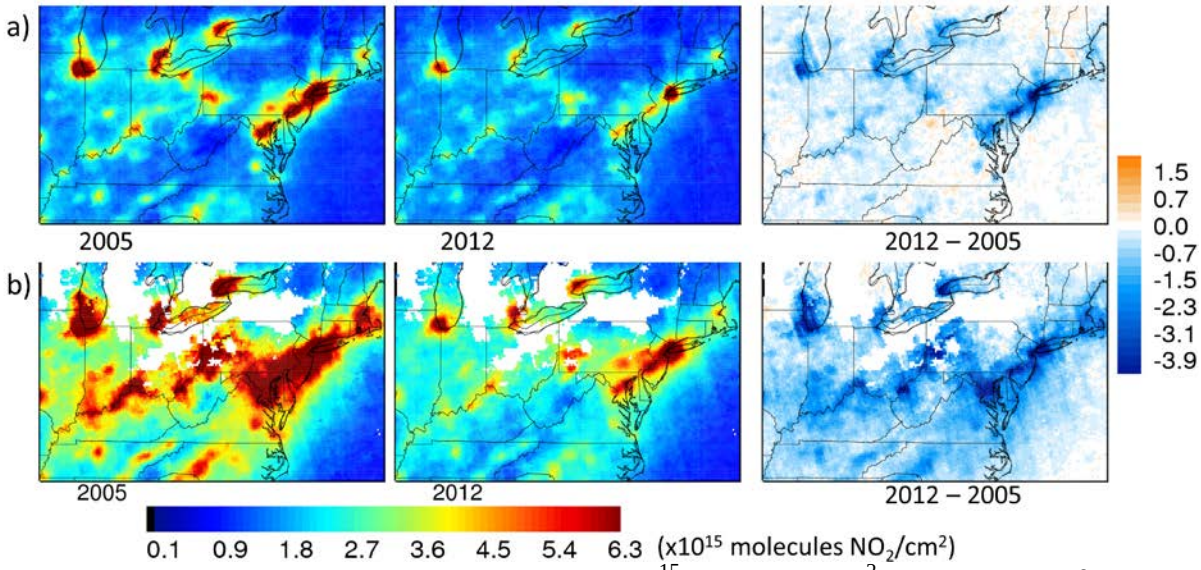

Figure 6. a) The OMI tropospheric NO_2 product (x10^{15} molecules/cm^2) as an average for the ozone season (May-September) in 2005 (left) and 2012 (middle) over the eastern U.S. The difference (x10^{15} molecules/cm^2) between the two years is also shown (right). b) The same as a), but as an annual average (January-December). In the left and middle panels, the white areas indicate regions where at least one month has three or less days of data with which to create the monthly averages, such as in winter with persistent snow and/or cloud cover.

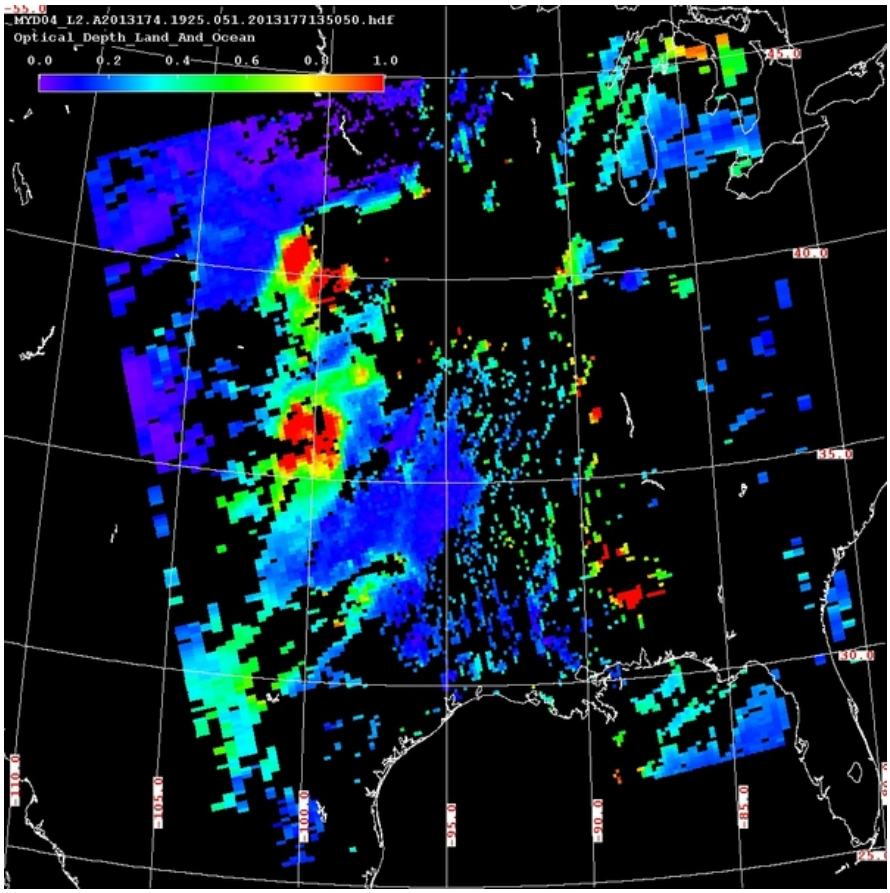

Figure 7. MODIS Level 2 image showing enhanced AOD levels due to fire activity in the central U.S. from the Level 1 and Atmosphere Archive and Distribution System (LAADS) Web tool (**Table 2**).

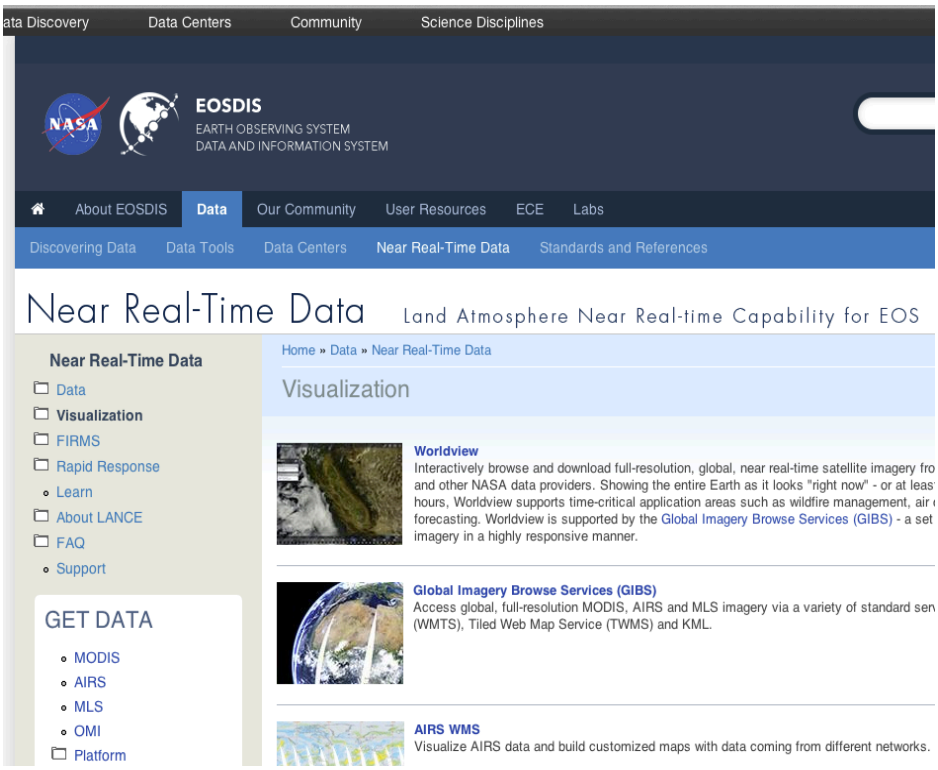

Figure 8. Interface of the EOSDIS LANCE web tool. As seen in the menu to the left, LANCE provides near-real-time data, including the capability of downloading data files and images, and number of visualization options relevant to AQ applications. Worldview, which can be accessed by clicking on the Visualization tab to the left, is a mapping interface where one or more images can be overlaid on a map, such as a MODIS true color image and an OMI NO_2 VCD image. The web tools allow the end-user to customize the images (**Table 2**).